



NUCLEAR ENERGY INSTITUTE

Alex Marion
DIRECTOR, ENGINEERING
NUCLEAR GENERATION DIVISION

September 26, 2003

Dr. Brian W. Sheron
Associate Director for Project Licensing and Technical Analysis
Office of Nuclear Reactor Regulation
U. S. Nuclear Regulatory Commission
Mail Stop O5-E7
Washington, DC 20555-00011

SUBJECT: Generic Relaxation Request for Order EA-03-009

PROJECT NUMBER: 689

Dear Dr. Sheron:

On June 12, 2003, representatives of the industry's Materials Reliability Project Alloy 600 Issues Task Group (ITG) met with staff from the Materials and Chemical Engineering Branch and the Office of Research to discuss industry activities related to various materials issues. During the meeting the staff reported that a number of plant specific relaxation requests had been received in response to Order EA-03-009 (Interim Inspection Requirements for Reactor Pressure Vessel Heads at Pressurized Water Reactors). The staff invited the industry to evaluate the areas of relaxation being requested and determine if a generic relaxation request would benefit both the industry and the NRC. The enclosed proposed change to the Order is our response to this suggestion.

The ITG's evaluation of the possible areas for relaxation revealed that many plants, when implementing the inspection requirements, found the specified extent of the nozzle examinations to be impractical because of limited clearances and other geometric conditions of their nozzles. Given that many of the PWRs have similar designs and thus similar configuration problems, the Alloy 600 ITG developed a proposed change to Order EA-03-009 that addresses such conditions. The ITG also developed a generic technical basis for the change that demonstrates no adverse effect on quality or safety.



The ITG's proposal would replace the italicized words in the following excerpt from Order EA-03-009...

- (a) Bare metal visual (BMV) examination of 100% of the RPV head surface (including 360° around each RPV head penetration nozzle), AND
- (b) Either:
 - (i) Ultrasonic testing of each RPV head penetration nozzle (i.e. nozzle base material) *from two (2) inches above the J-groove weld to the bottom of the nozzle and* complete an assessment to determine if leakage has occurred into the interference fit zone, OR
 - (ii) Eddy current testing or dye penetrant testing of the wetted surface of each J-groove weld and RPV head penetration nozzle base material *to at least two (2) inches above the J-groove weld.*

... with the italicized words in the excerpt below.

- (b) Bare metal visual (BMV) examination of 100% of the RPV head surface (including 360° around each RPV head penetration nozzle), AND
- (b) Either:
 - (i) Ultrasonic testing of each RPV head penetration nozzle (i.e. nozzle base material) *from 0.75" above the highest point of the root of the weld to 0.75" below the lowest point at the toe of the weld on the nozzle. For each RPV head penetration nozzle, also* complete an assessment to determine if leakage has occurred into the interference fit zone, OR
 - (ii) Eddy current testing or dye penetrant testing of the wetted surface of each J-groove weld and RPV head penetration nozzle base material *from 0.75" above the highest point of the root of the weld to 0.75" below the lowest point at the toe of the weld on the nozzle.*

The technical basis for this change is provided in EPRI report MRP-95, "Materials Reliability Program Generic Evaluation of Examination Coverage Requirements for Reactor Pressure Vessel Head Penetration Nozzles," Enclosure 1. This document shows that the proposed change maintains an acceptable level of quality and safety.

Dr. Brian W. Sheron
September 26, 2003
Page 3

Enclosure 1 contains proprietary information that is supported by the signed affidavit in Enclosure 2. The affidavit sets forth the basis on which the information may be withheld from public disclosure by the Commission and addresses with specificity the consideration listed in paragraph (b)(4) of Section 2.790 of the Commission's regulations. Accordingly, we respectfully request that the information, which is proprietary to EPRI, be withheld from public disclosure in accordance with 10 CFR 2.790. A non-proprietary version of the document is included in Enclosure 3.

Any NRC staff review of the enclosed information is exempt from the fee recovery provision contained in 10 CFR Part 170. This submittal provides information that might be helpful to NRC staff when evaluating licensee submittals provided in response to Order EA-03-009. Such reviews are exempted under §170.21, Schedule of Facility Fees. Footnote 4 to the Special Projects provision of §170.21 states, "Fees will not be assessed for requests/reports submitted to the NRC...as means of exchanging information between industry organizations and the NRC for the purpose of supporting generic regulatory improvements or efforts."

If there are any questions on these matters, please contact me (202-739-8080 or am@nei.org) or Jim Riley (202-739-8137 or jhr@nei.org).

Sincerely,



Alexander Marion

Enclosures

c: Mr. Bill Bateman, NRC
Mr. Terence Chan, NRC
Mr. Allen Hiser, NRC
Mr. William Cullen, NRC
Mr. Brian Benney, NRC

**Materials Reliability Program Generic Evaluation of
Examination Coverage Requirements for Reactor
Pressure Vessel Head Penetration Nozzles**

(MRP-95)

Proprietary Affidavit

September 24, 2003

Mr. Gene Carpenter
Document Control Desk
U.S. Nuclear Regulatory Commission
Washington, DC 20555

Subject: Request for Withholding of Proprietary Information Entitled, "*Materials Reliability Program: Generic Evaluation of Examination Coverage Requirements for Reactor Pressure Vessel Head Penetration Nozzles*" (MPR-95). EPRI Report ID 1009129

Dear Mr. Carpenter:

This is a request under 10CFR2.790(a)(4) that the NRC withhold from public disclosure the Information identified in the enclosed affidavit consisting of EPRI owned proprietary information as identified above (the "Information"). A copy of the Information and the affidavit in support of this request are enclosed.

EPRI desires to disclose the Information in confidence to the NRC for informational purposes to assist the NRC. EPRI would welcome any discussions with the NRC related to the Information that the NRC desires to conduct.

The Information is for the NRC's internal use and may be used only for the purposes for which it is disclosed by EPRI. The Information should not be otherwise used or disclosed to any person outside the NRC without prior written permission from EPRI.

If you have any questions about the legal aspects of this request for withholding, please do not hesitate to me at (650) 855-1073. Technical questions on the contents of the Information should be directed to Ms. Christine King at (650) 855-2605.

Sincerely,



Kevin Chu
Electric Power Research Institute, Inc.

Encls

cc: Ms. Christine King

AFFIDAVIT

RE: Request for Withholding of Proprietary Information Entitled, "*Materials Reliability Program: Generic Evaluation of Examination Coverage Requirements for Reactor Pressure Vessel Head Penetration Nozzles*" (MPR-95). EPRI Report ID 1009129

I, Kevin Chu, being duly sworn, depose and state as follows:

I am an Attorney at the Electric Power Research Institute, Inc. ("EPRI"), and I specifically have been delegated responsibility for the Information listed above that is sought under this affidavit to be withheld (the "Information") and authorized to apply for its withholding on behalf of EPRI. This affidavit is submitted to the Nuclear Regulatory Commission ("NRC") pursuant to 10 CFR 2.790 (a)(4) based on the fact that the Information consists of trade secrets of EPRI and that the NRC will receive the Information from EPRI under privilege and in confidence.

The basis for withholding such Information from the public is set forth below:

(1) The Information has been held in confidence by EPRI, its owner. All those accepting copies of the Information must agree to preserve the confidentiality of the Information.

(2) The Information is a type customarily held in confidence by EPRI and there is a rational basis therefor. The Information is a type that EPRI holds in confidence by means of a trade secret(s). This information is held in confidence by EPRI because disclosing it would prevent EPRI from licensing the Information and collecting royalties. Such royalty fees allow EPRI to recover its investment. If consultants and/or other businesses providing services in the electric/nuclear power industry were able to publicly obtain the Information, they would be able to use it commercially for profit and avoid spending the large amount of money that EPRI was required to spend in preparation of the Information. The rational basis that EPRI has for classifying the Information as a trade secret(s) is justified by the Uniform Trade Secrets Act, which California adopted in 1984 and which has been adopted by over twenty states. The Uniform Trade Secrets Act defines a "trade secret" as follows:

"Trade secret" means information, including a formula, pattern, compilation, program, device, method, technique, or process, that:

(i) Derives independent economic value, actual or potential, from not being generally known to the public or to other persons who can obtain economic value from its disclosure or use; and

(ii) Is the subject of efforts that are reasonable under the circumstances to maintain its secrecy.

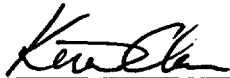
(3) The Information will be transmitted to the NRC in confidence.

(4) The Information is not available in public sources. EPRI developed the Information only after making a determination that the Information was not available from public sources. Developing the Information required a large expenditure of dollars and EPRI employees' time. The money spent, plus the value of EPRI's staff time in preparing the Information, shows that the Information is highly valuable to EPRI. Finally, the Information was developed only after a long period of effort of at least several months.

(5) A public disclosure of the Information would be highly likely to cause substantial harm to EPRI's competitive position and the ability of EPRI to license the Information both domestically and internationally. The Information can only be acquired and/or duplicated by others using an equivalent investment of time and effort.

I have read the foregoing, and the matters stated therein are true and correct to the best of my knowledge, information and belief. I make this affidavit under penalty of perjury under the laws of the United States of America and under the laws of the State of California.

Executed at 3412 Hillview Avenue, Palo Alto, California being the premises and place of business of the Electric Power Research Institute, Inc.

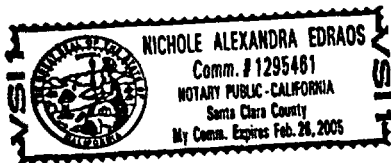


Kevin Chu

Subscribed and sworn before me this day: September 24, 2003



Nichole Alexandra Edraos, Notary Public



**Materials Reliability Program Generic Evaluation of
Examination Coverage Requirements for Reactor
Pressure Vessel Head Penetration Nozzles**

(MRP-95)

Non-Proprietary Version

**Materials Reliability Program
Generic Evaluation of Examination
Coverage Requirements for Reactor
Pressure Vessel Head Penetration
Nozzles (MRP-95NP)**

1009129

Topical Report, September 2003

**EPRI Project Manager
C. King**

DISCLAIMER OF WARRANTIES AND LIMITATION OF LIABILITIES

THIS DOCUMENT WAS PREPARED BY THE ORGANIZATION(S) NAMED BELOW AS AN ACCOUNT OF WORK SPONSORED OR COSPONSORED BY THE ELECTRIC POWER RESEARCH INSTITUTE, INC. (EPRI). NEITHER EPRI, ANY MEMBER OF EPRI, ANY COSPONSOR, THE ORGANIZATION(S) BELOW, NOR ANY PERSON ACTING ON BEHALF OF ANY OF THEM:

(A) MAKES ANY WARRANTY OR REPRESENTATION WHATSOEVER, EXPRESS OR IMPLIED, (I) WITH RESPECT TO THE USE OF ANY INFORMATION, APPARATUS, METHOD, PROCESS, OR SIMILAR ITEM DISCLOSED IN THIS DOCUMENT, INCLUDING MERCHANTABILITY AND FITNESS FOR A PARTICULAR PURPOSE, OR (II) THAT SUCH USE DOES NOT INFRINGE ON OR INTERFERE WITH PRIVATELY OWNED RIGHTS, INCLUDING ANY PARTY'S INTELLECTUAL PROPERTY, OR (III) THAT THIS DOCUMENT IS SUITABLE TO ANY PARTICULAR USER'S CIRCUMSTANCE; OR

(B) ASSUMES RESPONSIBILITY FOR ANY DAMAGES OR OTHER LIABILITY WHATSOEVER (INCLUDING ANY CONSEQUENTIAL DAMAGES, EVEN IF EPRI OR ANY EPRI REPRESENTATIVE HAS BEEN ADVISED OF THE POSSIBILITY OF SUCH DAMAGES) RESULTING FROM YOUR SELECTION OR USE OF THIS DOCUMENT OR ANY INFORMATION, APPARATUS, METHOD, PROCESS, OR SIMILAR ITEM DISCLOSED IN THIS DOCUMENT.

ORGANIZATION(S) THAT PREPARED THIS DOCUMENT

Structural Integrity Associates

ORDERING INFORMATION

Requests for copies of this report should be directed to EPRI Orders and Conferences, 1355 Willow Way, Suite 278, Concord, CA 94520, (800) 313-3774, press 2 or internally x5379, (925) 609-9169, (925) 609-1310 (fax).

Electric Power Research Institute and EPRI are registered service marks of the Electric Power Research Institute, Inc. EPRI. ELECTRIFY THE WORLD is a service mark of the Electric Power Research Institute, Inc.

Copyright © 2003 Electric Power Research Institute, Inc. All rights reserved.

CITATIONS

This report was prepared by

Structural Integrity Associates
6595 S. Dayton St. (Suite 3000)
Greenwood Village, CO 80111

Principal Investigator
P. Riccardella

This report describes research sponsored by EPRI.

The report is a corporate document that should be cited in the literature in the following manner:

Materials Reliability Program: Generic Evaluation of Examination Coverage Requirements for Reactor Pressure Vessel Head Penetration Nozzles (MRP-95NP), EPRI, Palo Alto, CA: 2003. 1009129.

PRODUCT DESCRIPTION

U.S. NRC Order EA-03-009—issued on February 11, 2003—requires specific examinations of reactor pressure vessel (RPV) upper vessel head penetration nozzles of all pressurized water (PWR) plants. Depending on an individual plant's susceptibility ranking, inspections are required at various intervals. When implementing these inspection requirements, a number of plants found the specified extent of the nozzle examinations to be impractical because of their nozzle clearances and other geometric conditions. Individual plants submitted alternate inspection examination zones to NRC, the NRC accepted these proposals that were shown to provide an acceptable level of quality and safety. This report contains a generic technical evaluation to determine a practical examination zone that will provide an acceptable level of quality and safety.

Results & Findings

Project results support an inspection zone in which the short sides are equal to 0.75 in. The long sides of the inspection zone are dependent on nozzle angle, but in all cases are bounded by horizontal scans encompassing the 0.75 in. short-side dimensions. The report establishes a reasonable target stress value (20 ksi), below which primary water stress corrosion cracking (PWSCC) is extremely remote. The report also demonstrates that in all but a few isolated cases the inspection zone envelopes all locations with stresses above this stress level. In no case does the examination zone exclude locations with stresses higher than 70% of the material yield strength. The report includes PWSCC growth calculations of postulated large flaws that could be overlooked due to unexamined regions to demonstrate that such flaws, either above or below the weld, would not grow to unacceptable sizes in several operating cycles.

Challenges & Objectives

This study's objective was to determine a practical examination zone that provides an acceptable level of quality and safety for all U.S. PWR RPV upper vessel head penetration nozzles.

Applications, Values & Use

The evaluation considers stresses in a group of characteristic plants that reasonably bound the fleet of U.S. PWRs from the standpoint of important factors that contribute to nozzle residual and operating stresses.

EPRI Perspective

This project has determined a practical examination zone for PWR RPV upper vessel head penetration nozzles that provides an acceptable level of quality and safety. A review of prior plant inspection data revealed that all flaws detected to date in top head nozzle exams in U.S.

PWRs would have been detected had the inspections been limited to just the proposed examination zones.

Approach

The project team developed plots of stress versus distance above and below the J-groove weld for several nozzles in four plants that reasonably bound the U.S. PWR fleet in terms of parameters that are expected to affect top head nozzle residual and operating stresses. The team then defined inspection zones, beyond which stresses decay significantly to levels at which PWSCC is considered highly unlikely. Then, assuming (non-mechanistically) that cracks form in the uninspected regions up to and impinging on the proposed inspection zones, the team performed fracture mechanics calculations to demonstrate that such cracks would not propagate to an unacceptable size for several operating cycles. These calculations were completed for plants of various RPV head designs and operating temperatures. Finally, nondestructive examination (NDE) data are reviewed and presented to demonstrate that in no case in which top head nozzle cracking has been detected would inspections of the proposed examination zones have missed such cracking.

Keywords

Primary water stress corrosion cracking

PWSCC

Alloy 600

Alloy 82/182

CRDM Nozzle

CEDM Nozzle

RPV Head penetration

J-groove weld

CONTENTS

1 INTRODUCTION	1-1
2 STRESS EVALUATION	2-1
2.1 Stress Limit for Examination Zone Definition	2-1
2.2 Characteristic Plants for Evaluation	2-3
2.3 Stress Plots and Determination of Limit Stress Distances	2-4
3 EXAMINATION ZONES	3-1
4 FRACTURE MECHANICS ANALYSES	4-1
4.1 Growth of Axial Cracks Below the Weld	4-1
4.2 Growth of Circumferential Cracks Above the Weld	4-7
5 COMPARISON TO PAST INSPECTION RESULTS	5-1
6 CONCLUSIONS	6-1
7 REFERENCES	7-1
A APPENDIX A	A-1
B APPENDIX B	B-1

LIST OF FIGURES

Figure 2-1 Typical pattern of RPV Top Head Nozzle Stresses Above and Below the J-Groove Weld (Steepest Angle Nozzle in a B&W-type Plant)	2-2
Figure 2-2 Comparison of Key Weld Geometry Variables Influencing Nozzle Residual Stresses – Plants Evaluated in this Study are Labeled.....	2-4
Figure 3-1 Schematic Illustration of Proposed Inspection Zone	3-2
Figure 3-2 Determination of Inspection Zone Distances needed to Envelope the > 20 ksi Stress Region for Figure 2-1 Stress Case (Steepest Angle Nozzle in B&W-type Plant).....	3-2
Figure 3-3 Inspection Zone Definitions based on >20 ksi Stress Limits for all Nozzles Analyzed	3-4
Figure 4-1 Illustration of Assumed Axial Flaw and Permissible Crack Growth Below the Weld Inspection Zone	4-2
Figure 4-2 Illustration of Assumed Circumferential Flaws Above the Weld Inspection Zone	4-2
Figure 4-3 Example of No Growth Case (Below Weld Axial Crack)	4-6
Figure 4-4 Example of Arrested Growth Case (Below Weld Axial Crack).....	4-6
Figure 4-5 Example of Growth Case (Below Weld Axial Crack)	4-7
Figure 4-6 Representative Circumferential Crack Growth Case Above Weld	4-11
Figure 4-7 Envelope Stresses Compared to Stresses at Edge of Inspection Zone	4-14
Figure 5-1 Flaw Area Outside of Weld.....	5-2
Figure A-1 Plant A (B&W) 38° Nozzle downhill Hoop Stress	A-1
Figure A-2 Plant A (B&W) 38° Nozzle downhill Axial Stress	A-2
Figure A-3 Plant A (B&W) 38° Nozzle sidehill Hoop Stress	A-2
Figure A-4 Plant A (B&W) 38° Nozzle sidehill Axial Stress.....	A-3
Figure A-5 Plant A (B&W) 38° Nozzle uphill Hoop Stress.....	A-3
Figure A-6 Plant A (B&W) 38° Nozzle uphill Axial Stress	A-4
Figure A-7 Plant A (B&W) 26° Nozzle downhill Hoop Stress	A-4
Figure A-8 Plant A (B&W) 26° Nozzle downhill Axial Stress.....	A-5
Figure A-9 Plant A (B&W) 26° Nozzle sidehill Hoop Stress	A-5
Figure A-10 Plant A (B&W) 26° Nozzle sidehill Axial Stress.....	A-6
Figure A-11 Plant A (B&W) 26° Nozzle uphill Hoop Stress.....	A-6
Figure A-12 Plant A (B&W) 26° Nozzle uphill Axial Stress	A-7
Figure A-13 Plant A (B&W) 18° Nozzle downhill Hoop Stress	A-7

Figure A-14 Plant A (B&W) 18° Nozzle downhill Axial Stress.....	A-8
Figure A-15 Plant A (B&W) 18° Nozzle sidehill Hoop Stress.....	A-8
Figure A-16 Plant A (B&W) 18° Nozzle sidehill Axial Stress.....	A-9
Figure A-17 Plant A (B&W) 18° Nozzle uphill Hoop Stress.....	A-9
Figure A-18 Plant A (B&W) 18° Nozzle uphill Axial Stress.....	A-10
Figure A-19 Plant A (B&W) 0° Nozzle downhill Hoop Stress.....	A-10
Figure A-20 Plant A (B&W) 0° Nozzle downhill Axial Stress.....	A-11
Figure A-21 Plant A (B&W) 0° Nozzle sidehill Hoop Stress.....	A-11
Figure A-22 Plant A (B&W) 0° Nozzle sidehill Axial Stress.....	A-12
Figure A-23 Plant A (B&W) 0° Nozzle uphill Hoop Stress.....	A-12
Figure A-24 Plant A (B&W) 0° Nozzle uphill Axial Stress.....	A-13
Figure A-25 Plant B (Westinghouse 2-loop) 43° Nozzle downhill Hoop Stress.....	A-13
Figure A-26 Plant B (Westinghouse 2-loop) 43° Nozzle downhill Axial Stress.....	A-14
Figure A-27 Plant B (Westinghouse 2-loop) 43° Nozzle sidehill Hoop Stress.....	A-14
Figure A-28 Plant B (Westinghouse 2-loop) 43° Nozzle sidehill Axial Stress.....	A-15
Figure A-29 Plant B (Westinghouse 2-loop) 43° Nozzle uphill Hoop Stress.....	A-15
Figure A-30 Plant B (Westinghouse 2-loop) 43° Nozzle uphill Axial Stress.....	A-16
Figure A-31 Plant B (Westinghouse 2-loop) 30° Nozzle downhill Hoop Stress.....	A-16
Figure A-32 Plant B (Westinghouse 2-loop) 30° Nozzle downhill Axial Stress.....	A-17
Figure A-33 Plant B (Westinghouse 2-loop) 30° Nozzle sidehill Hoop Stress.....	A-17
Figure A-34 Plant B (Westinghouse 2-loop) 30° Nozzle sidehill Axial Stress.....	A-18
Figure A-35 Plant B (Westinghouse 2-loop) 30° Nozzle uphill Hoop Stress.....	A-18
Figure A-36 Plant B (Westinghouse 2-loop) 30° Nozzle uphill Axial Stress.....	A-19
Figure A-37 Plant B (Westinghouse 2-loop) 13° Nozzle downhill Hoop Stress.....	A-19
Figure A-38 Plant B (Westinghouse 2-loop) 13° Nozzle downhill Axial Stress.....	A-20
Figure A-39 Plant B (Westinghouse 2-loop) 13° Nozzle sidehill Hoop Stress.....	A-20
Figure A-40 Plant B (Westinghouse 2-loop) 13° Nozzle sidehill Axial Stress.....	A-21
Figure A-41 Plant B (Westinghouse 2-loop) 13° Nozzle uphill Hoop Stress.....	A-21
Figure A-42 Plant B (Westinghouse 2-loop) 13° Nozzle uphill Axial Stress.....	A-22
Figure A-43 Plant B (Westinghouse 2-loop) 0° Nozzle downhill Hoop Stress.....	A-22
Figure A-44 Plant B (Westinghouse 2-loop) 0° Nozzle downhill Axial Stress.....	A-23
Figure A-45 Plant B (Westinghouse 2-loop) 0° Nozzle sidehill Hoop Stress.....	A-23
Figure A-46 Plant B (Westinghouse 2-loop) 0° Nozzle sidehill Axial Stress.....	A-24
Figure A-47 Plant B (Westinghouse 2-loop) 0° Nozzle uphill Hoop Stress.....	A-24
Figure A-48 Plant B (Westinghouse 2-loop) 0° Nozzle uphill Axial Stress.....	A-25
Figure A-49 Plant C (Westinghouse 4-loop) 48° Nozzle downhill Hoop Stress.....	A-25
Figure A-50 Plant C (Westinghouse 4-loop) 48° Nozzle downhill Axial Stress.....	A-26
Figure A-51 Plant C (Westinghouse 4-loop) 48° Nozzle sidehill Hoop Stress.....	A-26
Figure A-52 Plant C (Westinghouse 4-loop) 48° Nozzle sidehill Axial Stress.....	A-27

Figure A-53 Plant C (Westinghouse 4-loop) 48° Nozzle uphill Hoop Stress.....	A-27
Figure A-54 Plant C (Westinghouse 4-loop) 48° Nozzle uphill Axial Stress.....	A-28
Figure A-55 Plant D (CE) 49° Nozzle downhill Hoop Stress.....	A-28
Figure A-56 Plant D (CE) 49° Nozzle downhill Axial Stress.....	A-29
Figure A-57 Plant D (CE) 49° Nozzle sidehill Hoop Stress.....	A-29
Figure A-58 Plant D (CE) 49° Nozzle sidehill Axial Stress.....	A-30
Figure A-59 Plant D (CE) 49° Nozzle uphill Hoop Stress.....	A-30
Figure A-60 Plant D (CE) 49° Nozzle uphill Axial Stress.....	A-31
Figure A-61 Plant D (CE) 8° Nozzle downhill Hoop Stress.....	A-31
Figure A-62 Plant D (CE) 8° Nozzle downhill Axial Stress.....	A-32
Figure A-63 Plant D (CE) 8° Nozzle sidehill Hoop Stress.....	A-32
Figure A-64 Plant D (CE) 8° Nozzle sidehill Axial Stress.....	A-33
Figure A-65 Plant D (CE) 8° Nozzle uphill Hoop Stress.....	A-33
Figure A-66 Plant D (CE) 8° Nozzle uphill Axial Stress.....	A-34
Figure A-67 Plant D (CE) ICI Nozzle downhill Hoop Stress.....	A-34
Figure A-68 Plant D (CE) ICI Nozzle downhill Axial Stress.....	A-35
Figure A-69 Plant D (CE) ICI Nozzle sidehill Hoop Stress.....	A-35
Figure A-70 Plant D (CE) ICI Nozzle sidehill Axial Stress.....	A-36
Figure A-71 Plant D (CE) ICI Nozzle uphill Hoop Stress.....	A-36
Figure A-72 Plant D (CE) ICI Nozzle uphill Axial Stress.....	A-37
Figure B-1 Inspection Zone Distances that Envelopes > 20 ksi Stress Regions Plant A (B&W) 38° Nozzle.....	B-1
Figure B-2 Inspection Zone Distances that Envelopes > 20 ksi Stress Regions Plant A (B&W) 26° Nozzle.....	B-2
Figure B-3 Inspection Zone Distances that Envelopes > 20 ksi Stress Regions Plant A (B&W) 18° Nozzle.....	B-2
Figure B-4 Inspection Zone Distances that Envelopes > 20 ksi Stress Regions Plant A (B&W) 0° Nozzle.....	B-3
Figure B-5 Inspection Zone Distances that Envelopes > 20 ksi Stress Regions Plant B (Westinghouse 2-loop) 43° Nozzle.....	B-3
Figure B-6 Inspection Zone Distances that Envelopes > 20 ksi Stress Regions Plant B (Westinghouse 2-loop) 30° Nozzle.....	B-4
Figure B-7 Inspection Zone Distances that Envelopes > 20 ksi Stress Regions Plant B (Westinghouse 2-loop) 13° Nozzle.....	B-4
Figure B-8 Inspection Zone Distances that Envelopes > 20 ksi Stress Regions Plant B (Westinghouse 2-loop) 0° Nozzle.....	B-5
Figure B-9 Inspection Zone Distances that Envelopes > 20 ksi Stress Regions Plant C (Westinghouse 4-loop) 48° Nozzle.....	B-5
Figure B-10 Inspection Zone Distances that Envelopes > 20 ksi Stress Regions Plant D (CE) 49° Nozzle.....	B-6
Figure B-11 Inspection Zone Distances that Envelopes > 20 ksi Stress Regions Plant D (CE) 8° Nozzle.....	B-6

LIST OF TABLES

Table 3-1 Stresses at 0.75 in. for Nozzles that Violate the 20 ksi Criteria	3-3
Table 4-1 Starting Flaw Lengths for Crack Growth Analysis of Postulated Axial Cracks below J-Groove Welds	4-3
Table 4-2 PWSCC Crack Growth Correlations vs. Temperature for Above Weld Annulus Region (including severe environmental factor of 2)	4-4
Table 4-3 Crack Growth Times for Postulated Axial Cracks at Edge of Below Weld Inspection Zone to Reach Weld (Minimum Time is Greater than Five EFPYs)	4-5
Table 4-4 Stress Intensity Factor for Above-Weld Circumferential Flaws for Plant A (B&W Type Plant - Envelop Stress Distributions)	4-8
Table 4-5 Stress Intensity Factor for Above-Weld Circumferential Flaws for Plant B (W 2- Loop Plant - 43.5° Nozzle - Envelop Stress Distributions)	4-8
Table 4-6 Stress Intensity Factor for Above-Weld Circumferential Flaws for Plant C (W 4- Loop Plant – 48.8° Nozzle - Envelop Stress Distributions)	4-9
Table 4-7 Stress Intensity Factor for Above-Weld Circumferential Flaws for Plant D (CE Plant – 49.7° Nozzle - Envelop Stress Distributions)	4-9
Table 4-8 Flaw Length Correlations, Degrees and Inches, For Limiting Nozzles	4-10
Table 4-9 Growth Time from 30° to 300° Circumferential Crack Plant A - 38° Nozzle	4-12
Table 4-10 Growth Time from 30° to 300° Circumferential Crack Plant B – 43.5° Nozzle.....	4-12
Table 4-11 Growth Time from 30° to 300° Circumferential Crack Plant C – 48.8° Nozzle	4-13
Table 4-12 Growth Time from 30° to 300° Circumferential Crack Plant D – 49.7° Nozzle	4-13

1

INTRODUCTION

U.S. NRC Order EA-03-009 issued on February 11, 2003 requires specific examinations of the reactor pressure vessel (RPV) top head and vessel head penetration nozzles of all pressurized water (PWR) plants. In accordance with the order, inspections are required to be performed at various intervals, depending on the susceptibility ranking of the individual plants. The required inspections consist of:

- (a) Bare metal visual (BMV) examination of 100% of the RPV head surface (including 360° around each RPV head penetration nozzle), AND
- (b) Either:
 - (i) Ultrasonic testing of each RPV head penetration nozzle (i.e. nozzle base material) from two (2) inches above the J-groove weld to the bottom of the nozzle and an assessment to determine if leakage has occurred into the interference fit zone, OR
 - (ii) Eddy current testing or dye penetrant testing of the wetted surface of each J-groove weld and RPV head penetration nozzle base material to at least two (2) inches above the J-groove weld.

A number of plants, when implementing these inspection requirements, found the specified extent of the nozzle examinations to be impractical because of clearances and other geometric conditions of their nozzles. They proposed, and the NRC accepted, alternative examination zones which were shown to provide an acceptable level of quality and safety.

This report contains a generic technical evaluation to determine a practical examination zone which will provide an acceptable level of quality and safety. It addresses extent of examination both above the top and below the bottom of the J-groove weld. The evaluation considers stresses in a group of characteristic plants that reasonably bound the fleet of U.S. PWRs from the standpoint of the important factors that contribute to nozzle residual and operating stresses. Plots of stress versus distance above and below the J-groove weld are developed for several nozzles in these plants. Inspection zones are then defined, beyond which the stresses decay significantly, to levels at which primary water stress corrosion cracking (PWSCC) is considered highly unlikely. Then, assuming (non-mechanistically) that cracks form in the uninspected regions up to and impinging upon the proposed inspection zones, fracture mechanics calculations are performed to demonstrate that such cracks would not propagate to an unacceptable size for several operating cycles in plants of various RPV head designs and operating temperatures. Finally, NDE data are reviewed and presented to demonstrate the effectiveness of the proposed examination zone with respect to prior inspection results for U.S. PWR top head nozzles.

Introduction

The results of this evaluation support an inspection zone, illustrated schematically in Figure 3-1 of this report, in which the short sides (a_{up} and b_{dn} in Fig. 3-1) are equal to 0.75 in. The long sides of the inspection zone (a_{dn} and b_{up} in Fig. 3-1) are dependent on nozzle angle, but in all cases are bounded by horizontal scans encompassing the 0.75 in. short side dimensions. The report establishes a reasonable target stress value (20 ksi), below which PWSCC is extremely remote, and demonstrates that in all but a few isolated cases, the inspection zone, as defined above, envelopes all locations with stresses above this stress level. In no case does the examination zone exclude locations with stresses higher than 70% of the material yield strength. The report also includes PWSCC growth calculations of postulated large flaws that could be overlooked due to unexamined regions, to demonstrate that such flaws, either above or below the weld, would not grow to unacceptable sizes in several operating cycles. Finally, review of prior plant inspection data from a large cross-section of U.S. PWRs revealed that, of 237 flaw indications reported in these inspections, all flaws would have been detected had the inspections been limited to just the proposed examination zones.

2

STRESS EVALUATION

2.1 Stress Limit for Examination Zone Definition

PWSCC in RPV head nozzles occurs due to a combination of susceptible materials, environment and high stress levels. In the vicinity of the J-groove welds, where the cracking has been observed, high stresses generally exist due to welding residual stresses, plus a small contribution from operating thermal and pressure stresses. Typical plots of operating plus residual stresses for a top head penetration nozzle are illustrated in Figure 2-1. This figure presents hoop stresses on the nozzle inside and outside surfaces, as a function of axial distance from the bottom of the nozzle (located at 64.5 inches on the horizontal axis). The upper chart (a) is for the uphill side of the nozzle, while the lower plot (b) is for the downhill side. Weld locations are identified by rectangular boxes on these charts. It is seen from this figure that the stresses peak at values on the order of 80 ksi directly under the welds, but that they attenuate rapidly with distance either above or below the weld.

In order to determine a practical examination zone, which will ensure an acceptable level of quality and safety, it is desirable to define a stress limit below which there is a very low probability of initiating PWSCC cracks. There is fairly universal agreement that high stresses, on the order of the material yield strength, are necessary to initiate PWSCC. Reference 1 states "there is no known case of stress corrosion cracking of Alloy-600 below the yield stress." Typical yield strengths for wrought Alloy-600 head penetration nozzles are in the range of 37 ksi to 65 ksi. (The ASME Code minimum yield strength is 35 ksi for SB-166 material, and 30 ksi for SB-167 hot worked tube material.) Weld metal yield strengths are generally higher. For purposes of this evaluation, a target stress level of 20 ksi has been selected as a safe value, below which PWSCC initiation is very unlikely. However, a stress equal to the material yield strength is arguably the absolute minimum necessary for PWSCC, and in a few locations, a limit equal to 70% of the yield strength used in the residual stress calculations has been applied.

Reference 2 presents the following relationship for PWSCC time to crack initiation:

$$t_f = (C/I_m) \sigma^{-4} \exp(E/RT)$$

where: t_f = failure time

C = a constant

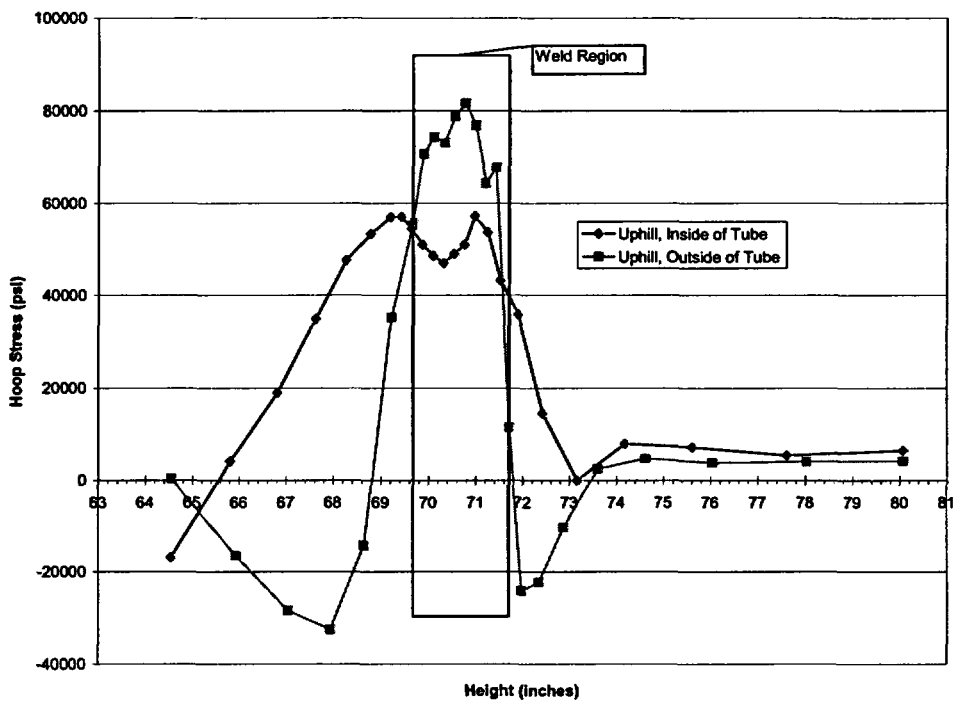
σ = applied stress

I_m = material susceptibility index

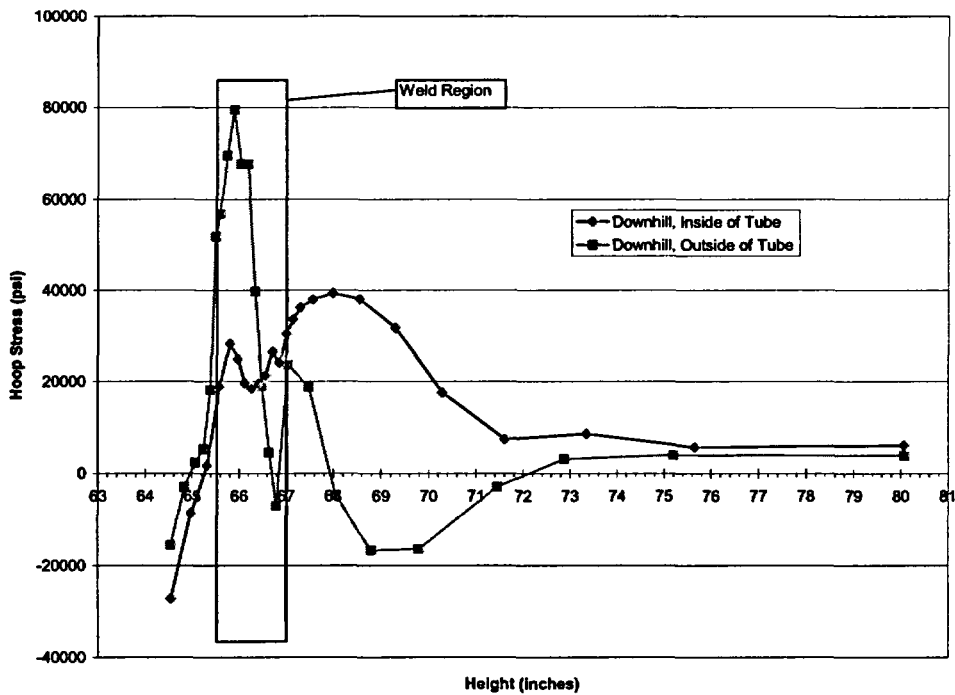
R = activation energy

E = universal gas constant

T = absolute temperature



(a) Uphill Side of Nozzle



(b) Downhill side of Nozzle

Figure 2-1
 Typical pattern of RPV Top Head Nozzle Stresses Above and Below the J-Groove Weld
 (Steepest Angle Nozzle in a B&W-type Plant)

In accordance with this relationship, time to failure (i.e. crack initiation) is proportional to stress to the power of -4. Assuming that all of the observed stress corrosion cracking to date has been at stresses greater than the material yield strength, the stress limit of 70% of yield strength equates to greater than a four-fold increase in time to cracking.

2.2 Characteristic Plants for Evaluation

A group of characteristic plants have been selected for evaluation that reasonably bound the U.S. PWR fleet in terms of parameters that are expected to affect top head nozzle residual and operating stresses. The specific plant types selected are:

- Plant A – A typical B&W type plant with nozzle angles ranging from 0° to 38°, and reported nozzle yield strengths ranging from 36.8 to 50 ksi. [3]
- Plant B – A Westinghouse 2-loop plant with nozzle angles ranging from 0° to 43.5°, and reported nozzle yield strength of 58 ksi. [4]
- Plant C – A Westinghouse 4-loop plant with nozzle angles ranging from 0° to 48.8°, and reported nozzle yield strength of 63 ksi. [5]
- Plant D – A large CE type plant with CEDM nozzle angles ranging from 0° to 49.7°, and reported nozzle yield strengths ranging from 52.5 to 59 ksi. This plant also contained ICI nozzles with a 55.3° nozzle angle and a yield strength of 39.5 ksi.[6]

In addition to nozzle angle and yield strength, an important factor influencing residual stress is the weld geometry. Figure 2-2 summarizes a wide range of PWR top head nozzle geometries which have been previously analyzed. Plotted on the horizontal axis of this chart is the average J-groove weld cross-sectional area for each of the plants, distinguished by ranges of nozzle angle. Plotted on the vertical axis is the ratio of uphill to downhill weld cross-sectional area for the same nozzles. In general, the larger the weld size, the higher the residual stress one would expect. The ratio of uphill to downhill weld areas is also expected to effect the distribution of stress around the nozzle, and the stress attenuation with distance from the weld. Data points representing the steepest angle nozzles in the four characteristic plant types listed above are labeled in this chart. It is seen from Figure 2-2 that the four plants selected are reasonable bounds to the complete collection of points. Plant B represents the largest average weld size in the group, and also has relatively high yield strength. Plants A and C have about average weld sizes but span the range of uphill to downhill weld size ratios, from the highest (uphill weld area almost twice that of the downhill weld) to the lowest (downhill weld area more than twice that of the uphill weld). Plant D is somewhat central to the group, both in terms of average weld size and ratio. This group of plants also spans a wide range of nozzle yield strengths, from 36.8 ksi to 63 ksi. In addition to the highest angle nozzles for each plant, the evaluation also addresses selected intermediate and low angle welds from several of the plant types, as well as ICI nozzles in the CE type plant, to cover a range of the other data symbols in Figure 2-2.

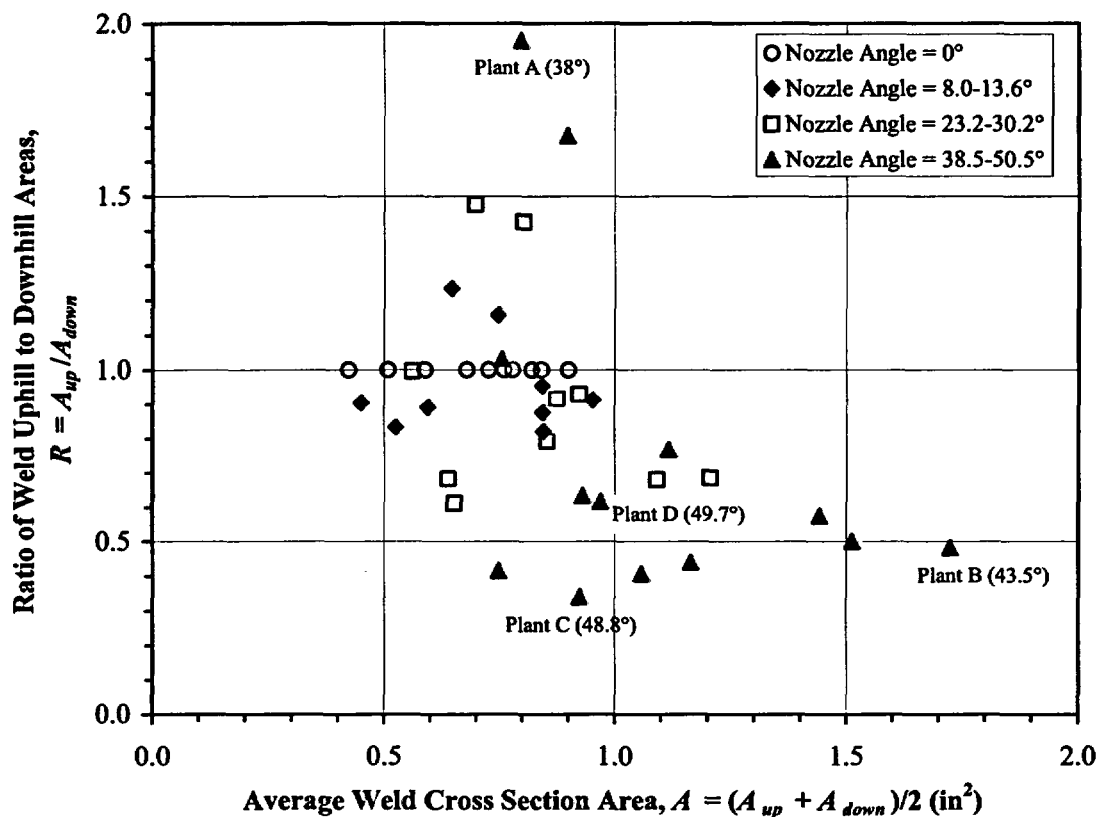


Figure 2-2
 Comparison of Key Weld Geometry Variables Influencing Nozzle Residual Stresses –
 Plants Evaluated in this Study are Labeled

The conclusion from this section is that the characteristic plants selected for evaluation bound the fleet of U.S. plants in terms of weld geometries and yield strengths, and that the resulting examination zone is therefore applicable to all U.S. PWRs.

2.3 Stress Plots and Determination of Limit Stress Distances

Stress plots similar to Figure 2-1 have been obtained from prior calculations [3 – 6] for the maximum angle nozzle in each of the four characteristic plants, as well as for several intermediate angle nozzles from the characteristic plants. The complete series of plots, including hoop and axial stresses for uphill, sidehill, and downhill locations in each nozzle are compiled in Appendix A. These plots were used to determine the distances above and below the weld at which the stress decays to below the 20 ksi limit. The results are summarized and used as the basis for defining an examination zone in Section 3 below.

3

EXAMINATION ZONES

Figure 2-1 exhibits a pattern that is repeated in essentially all of the stress plots in Appendix A. On the uphill side of an angled nozzle (Figure 2-1a), the stresses decay more rapidly above the weld than below the weld (i.e. the stress rise is skewed downward from the weld). Conversely, on the downhill side (Figure 2-1b), the stresses decay more rapidly below the weld (i.e. the stress rise is skewed upward). This trend, seen in virtually all of the nozzles evaluated, is more pronounced in the steeper angled nozzles, gradually decreasing with nozzle angle. The only exception is the zero angled nozzles, for which the stress rise is symmetric, since there is no uphill or downhill in these nozzles.

This pattern leads to a general expectation regarding the nature of the inspection zone necessary to envelope any given stress limit. As illustrated schematically in Figure 3-1, the inspection zone will be bounded by four linear dimensions:

a_{up} – the required inspection distance above the weld on the uphill side

a_{dn} – the required inspection distance above the weld on the downhill side

b_{up} – the required inspection distance below the weld on the uphill side

b_{dn} – the required inspection distance below the weld on the downhill side

Because of the previously described asymmetry of the stress distributions, it is expected that a_{up} will be less than a_{dn} and b_{dn} will be less than b_{up} . To determine appropriate values of these inspection distances, the plots in Appendix A have been assessed to determine the lengths in each nozzle at which the stresses drop below 20 ksi (denoted by vertical lines in the Appendix A plots). These were used to construct plots similar to Figure 3-2, which is the inspection zone definition resulting from the stress plots of Figure 2-1 (Steepest Angle Nozzle in a B&W-type Plant). The solid lines with data points represent the distances above and below the weld at which the axial or hoop stress drops below 20 ksi. The heavy chain-link lines represent the resulting inspection zone for this nozzle which envelopes the >20 ksi stress region. In this case:

$$a_{up} = 0.75 \text{ in.}$$

$$a_{dn} = 3.4 \text{ in.}$$

$$b_{up} = 3.4 \text{ in.}$$

$$b_{dn} = 0.75 \text{ in.}$$

Note that in Figure 3-2, distances above the top of weld are plotted as positive and distances below the bottom of the weld are plotted as negative.

Examination Zones

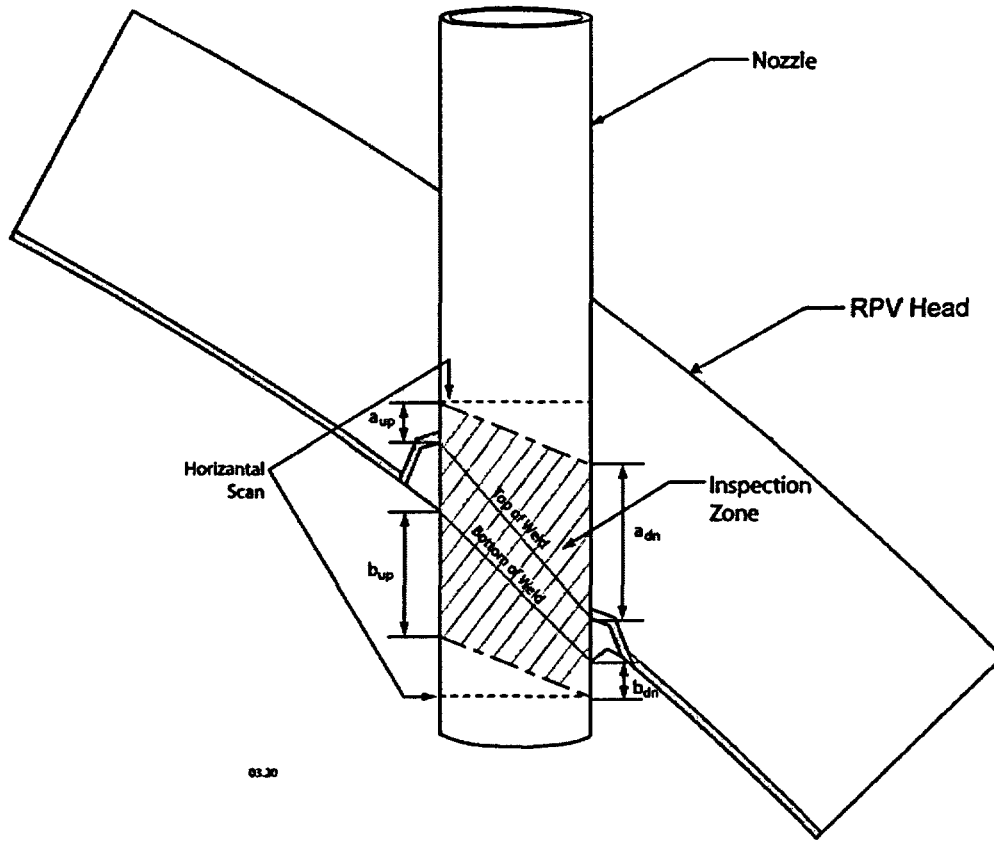


Figure 3-1
Schematic Illustration of Proposed Inspection Zone

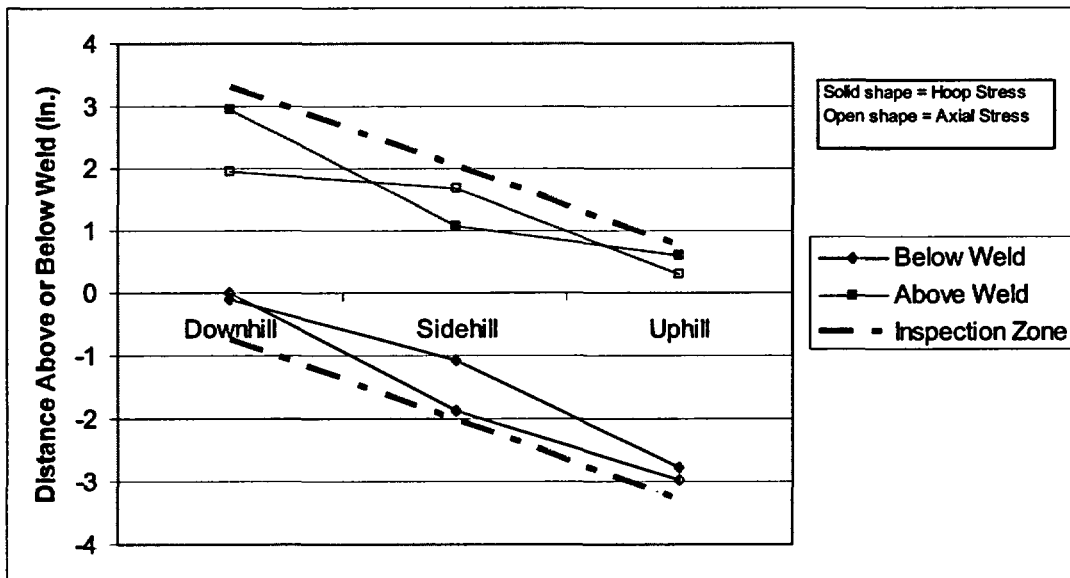


Figure 3-2
Determination of Inspection Zone Distances needed to Envelope the > 20 ksi Stress Region for Figure 2-1 Stress Case (Steepest Angle Nozzle in B&W-type Plant)

Similar plots were constructed for all of the nozzles analyzed, a compilation of which is contained in Appendix B. The results are summarized in Figure 3-3, in terms of inspection distances above and below the weld as a function of nozzle angle. Figure 3-3 illustrates that, for nozzle angles greater than around 15°, the >20 ksi stress regime is reasonably bounded by 0.75 in. on the short side (a_{up} and b_{dn}). For smaller nozzle angles, and for one 30° nozzle, the lengths at which the stress drops below 20 ksi are somewhat greater than 0.75 in., on the order of 1 to 1.2 in. However, as listed in Table 3-1, the stresses in these nozzles at 0.75 in. remains lower than 70% of the nozzle yield strength used in the residual stress calculation. (In fact, in all but one case it remains below 60% of yield strength.) Thus, even though the stresses in these cases would exceed the 20 ksi stress level, at 0.75 in., the 0.75 in. inspection zone is sufficient to bound all regions with any probability of initiating PWSCC in a plant lifetime.

Table 3-1
Stresses at 0.75 in. for Nozzles that Violate the 20 ksi Criteria

Nozzle Angle	Stress at 0.75 in.		Yield Strength (ksi)	Ratio Max. @ 0.75" / YS
	Hoop (ksi)	Axial (ksi)		
0°	29	29	50	.58
0°	32	34	58	.59
8°	33	29	59	.56
13°	41	37	58	.7
30°	33.5	32	58	.58
55° (ICI)	22.5	Compressive	39.5	.57

On the long side (a_{dn} and b_{up}), the 20 ksi stress limit is reasonably bounded by a linear function of nozzle angle, varying from 1 in. at zero degrees to 4.25 inches at 50°. For inspection processes which control scans in both the vertical and horizontal directions, the long sides of the inspection zone are as shown in Figure 3-3b and can be approximated by the following equations:

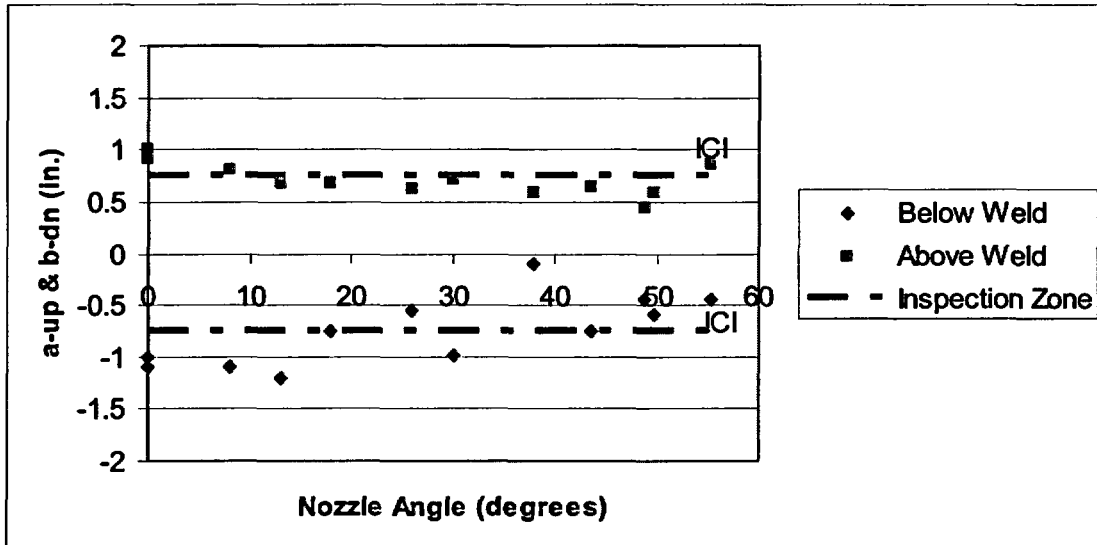
$$a_{dn} = .75 + 3.5\alpha / 50^\circ$$

$$b_{up} = .75 + 3.5\alpha / 50^\circ$$

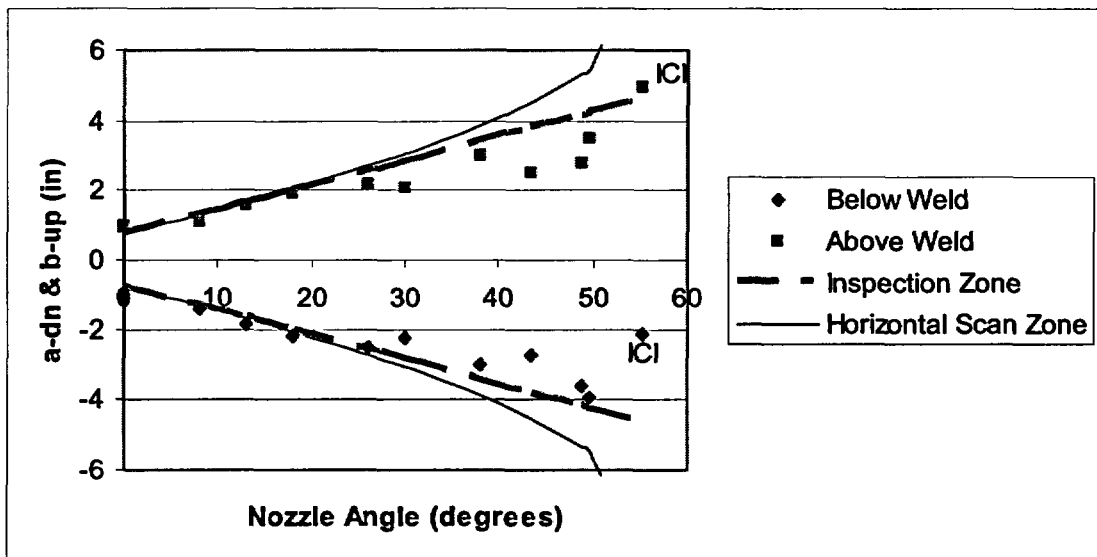
where: α = the nozzle angle in degrees.

Also illustrated in Figure 3-3b is a horizontal scan zone encompassing a_{up} and $b_{dn} = 0.75$ in. It is seen that a horizontal scan bounds the required long-side inspection zone at all nozzle angles. Thus, if an inspection process uses a horizontal scan pattern for the inspections, the only inspection zone requirement is that a_{up} and b_{dn} satisfy the 0.75 in. criteria noted above. (The discontinuity in the horizontal scan line of Figure 3-3b reflects the fact that the ICI nozzles are of

larger diameter, and the horizontal scan therefore encompasses more length on these nozzles than for the CRDM/CEDM nozzles.)



a) Short Side Dimension of Inspection Zone (a_{up} and b_{dn})



b) Long Side Dimension of Inspection Zone (a_{dn} and b_{up})
- Horizontal Scan Pattern also Shown

Figure 3-3
Inspection Zone Definitions based on >20 ksi Stress Limits for all Nozzles Analyzed

4

FRACTURE MECHANICS ANALYSES

As further confirmation that the inspection zones defined in Section 3 provide an acceptable level of quality and safety, fracture mechanics calculations have also been performed to demonstrate that flaws which would be missed because they are just outside of the inspection zone would not grow to unacceptable sizes during at least one fuel cycle of plant operation. Calculations are performed for axially oriented flaws in the nozzle end just below the inspection zone (Figure 4-1), as well as for circumferential flaws just above the inspection zone (Figure 4-2).

4.1 Growth of Axial Cracks Below the Weld

The portion of the CRDM/CEDM tubes that extend into the reactor vessel is exposed to reactor water chemistry, and is thus potentially susceptible to PWSCC. The stresses that would drive such cracking are expected to be much lower than in the vicinity of the annulus or J groove weld, however, since internal and external pressure is the same, and since this portion of the tube is, for the most part, remote from the high residual stresses associated with the J-groove weld.

Assuming an examination zone as proposed in Section 3, the limiting flaw that could remain undetected in the portion of the tube under the J-groove weld is postulated to be a through-wall axial flaw propagating from the bottom of the tube upward to the lower edge of the examination zone (see Figure 4-1). If such a flaw were to grow to the bottom of the J-groove weld, it could potentially lead to leakage, since crack propagation in the weld metal is expected to be faster than in the Alloy-600 base metal.

To demonstrate that the proposed inspection zones provide adequate protection against leakage, a series of deterministic fracture mechanics calculations were performed. The assumed initial flaw length is different for different plant types and locations, as shown in Table 4-1. Analyses were done for the downhill, sidehill, and uphill locations for the most limiting CRDM/CEDM penetration (i.e., the steepest nozzle angle) for each of the limiting plant types. Analysis details are contained in Ref. [14].

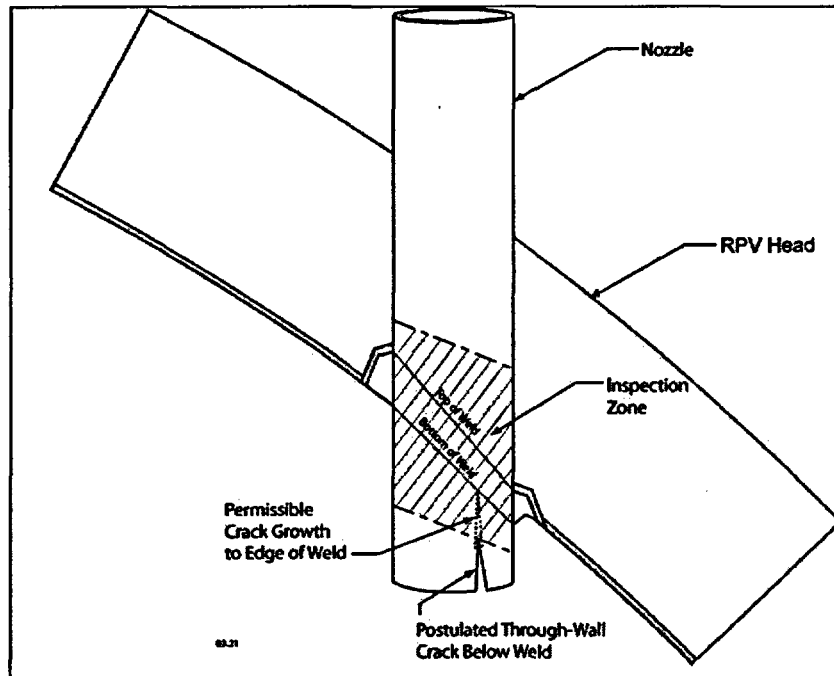


Figure 4-1
Illustration of Assumed Axial Flaw and Permissible Crack Growth Below the Weld
Inspection Zone

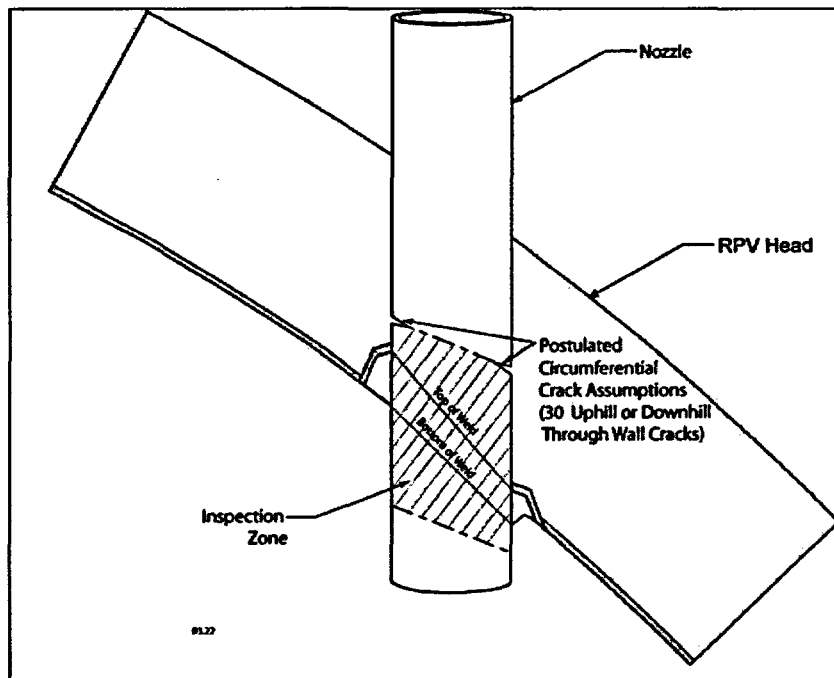


Figure 4-2
Illustration of Assumed Circumferential Flaws Above the Weld
Inspection Zone

Table 4-1
Starting Flaw Lengths for Crack Growth Analysis of Postulated Axial Cracks below J-Groove Welds

PLANT/NOZZLE	LOCATION	LENGTH (in. from bottom of nozzle to weld)	INSPECTION ZONE (in. below weld)	STARTING FLAW SIZE (in.)
Plant A	DOWNHILL	1.053	0.75	0.303
(B&W 38°)	SIDEHILL	3.122	2.025	1.097
	UPHILL	5.132	3.3	1.832
Plant B	DOWNHILL	1.917	0.75	1.167
(W 2-LOOP 43.5°)	SIDEHILL	3.537	2.175	1.362
	UPHILL	5.104	3.600	1.504
Plant C	DOWNHILL	2.134	0.75	1.384
(W 4-LOOP 48.8°)	SIDEHILL	4.437	2.200	2.237
	UPHILL	6.650	3.900	2.750
Plant D	DOWNHILL	2.498	0.75	1.748
(CE 49.7°)	SIDEHILL	5.050	2.375	2.675
	UPHILL	7.490	4.000	3.490

Stresses for these analyses are taken from the stress distributions described in Section 2, and compiled in Appendix A. Specifically, hoop stress distributions (which would tend to open axial flaws in the tubes) were selected for the inside and outside of each limiting tube for each azimuth. These stresses include weld residual stresses, pressure stresses, and any other sustained applied loads affecting the hoop direction.

For conservatism and ease of calculation, the hypothetical axial cracks were modeled for fracture mechanics analyses as edge-connected through-wall cracks in a wide flat plate. This model does not account for the hoop constraint of the actual geometry, and therefore is conservative compared to the actual geometry.

The stress results were input to the SI fracture mechanics program **pc-CRACK** [7] to calculate the applied stress intensity factor (K_{applied}) distribution for each case. K was determined for crack lengths spanning the complete length of each tube from the bottom-most edge, to the start of the J-Groove weld. K was determined as a function of distance from the bottom edge of the tube, for each plant type, for downhill, sidehill, and uphill flaw locations.

Flaw growth rate correlations were determined for these assumed flaw locations as a function of temperature, using the methods of MRP-55 [8]. For the purpose of the present analysis, various temperatures ranging from 580 F to 605 F were assumed. This results in a crack growth correlation of

$$da/dt = A (K_{\text{applied}} - K_{\text{threshold}})^{1.16} \text{ inch/hour}$$

where:

A = ID coefficient from Table 4-2

K_{applied} = the K distribution as determined above

$K_{\text{threshold}}$ = 8.19 ksi- $\sqrt{\text{in}}$

Crack growth calculations were performed for the assumed initial flaw sizes, using the K distributions and this crack growth correlation. Results are shown in Table 4-3. This table shows that, for more than half of the cases studied, the applied K at the assumed initial flaw size (just impinging on the inspection zone) does not exceed the threshold stress intensity factor value, and consequently for these cases, no flaw growth is predicted. In one case, the initial applied K is above the threshold value (allowing growth) but the applied K drops below the threshold after a short period of growth, so the initial flaw is expected to arrest its growth before reaching the weld. In the remaining several cases, continuing growth is predicted, and the growth time required to reach the J groove weld is included in the table. The minimum crack growth time reported in Table 4-3 is 46,000 hours, which corresponds to over four EFPYs at a 605 F operating temperature. Operation at lower temperatures results in even longer times. Representative crack growth plots for these three cases, respectively, are illustrated in Figures 4-3, 4-4 and 4-5.

Table 4-2
**PWSCC Crack Growth Correlations vs. Temperature for Above Weld Annulus Region
 (Including severe environmental factor of 2)**

TEMPERATURE (°F)	COEFFICIENT (ID)	COEFFICIENT (ANNULUS)	EXPONENT
605	3.40 E-07	6.80 E-07	1.16
602	3.15 E-07	6.32 E-07	1.16
600	3.00 E-07	6.01 E-07	1.16
595	2.65 E-07	5.30 E-07	1.16
590	2.33 E-07	4.67 E-07	1.16
585	2.05 E-07	4.11 E-07	1.16
580	1.80 E-07	3.61 E-07	1.16

**Table 4-3
Crack Growth Times for Postulated Axial Cracks at Edge of Below Weld Inspection Zone to Reach Weld (Minimum Time Is Greater than Five EFPYs)**

PLANT/NOZZLE	LOCATION	K @ STARTING FLAW SIZE (KSI-√IN)	CRACK GROWTH TIME TO BOTTOM OF WELD (HRS)				
			580° F	590° F	600° F	602° F	605° F
Plant A (B&W 38°)	DOWNHILL	< 8.19	No Growth	No Growth	No Growth	No Growth	No Growth
	SIDEHILL	< 8.19	No Growth	No Growth	No Growth	No Growth	No Growth
	UPHILL	< 8.19	No Growth	No Growth	No Growth	No Growth	No Growth
Plant B (W 2-LOOP 43.5°)	DOWNHILL	< 8.19	No Growth	No Growth	No Growth	No Growth	No Growth
	SIDEHILL	38.4	101000	78000	61000	58000	54000
	UPHILL	< 8.19	No Growth	No Growth	No Growth	No Growth	No Growth
Plant C (W 4-LOOP 48.8°)	DOWN	9.54	92000	71000	55600	53000	49000
	SIDE	< 8.19	No Growth	No Growth	No Growth	No Growth	No Growth
	UP	16	Arrests	Arrests	Arrests	Arrests	Arrests
Plant D (CE 49.7°)	DOWN	10	87000	67000	53000	50000	46000
	SIDE	46.2	122000	94000	74000	70000	65000
	UP	< 8.19	No Growth	No Growth	No Growth	No Growth	No Growth

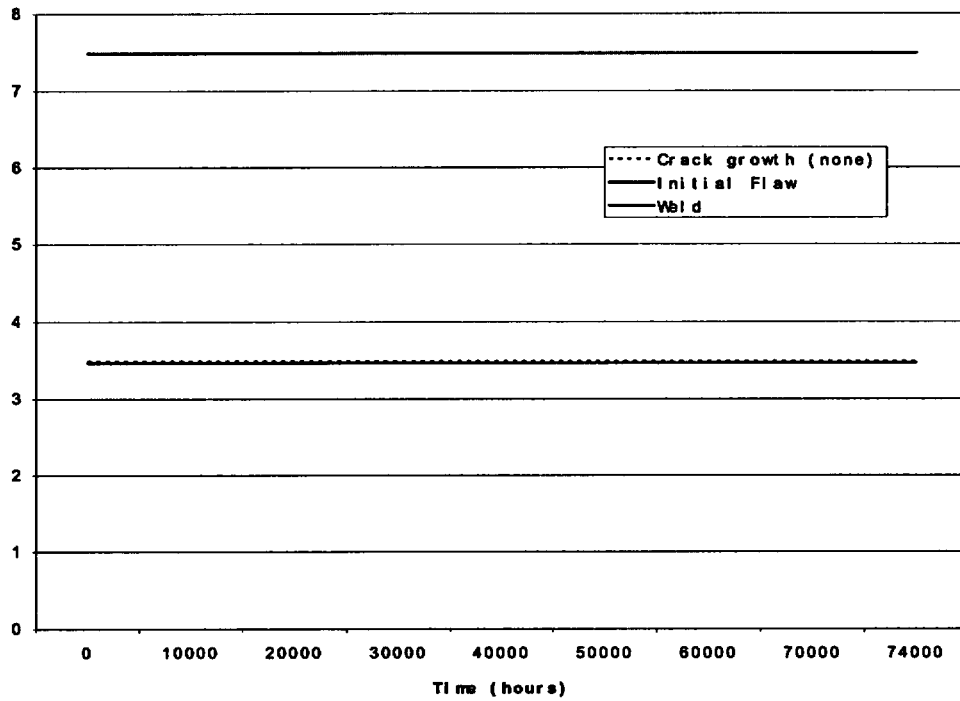


Figure 4-3
Example of No Growth Case (Below Weld Axial Crack)

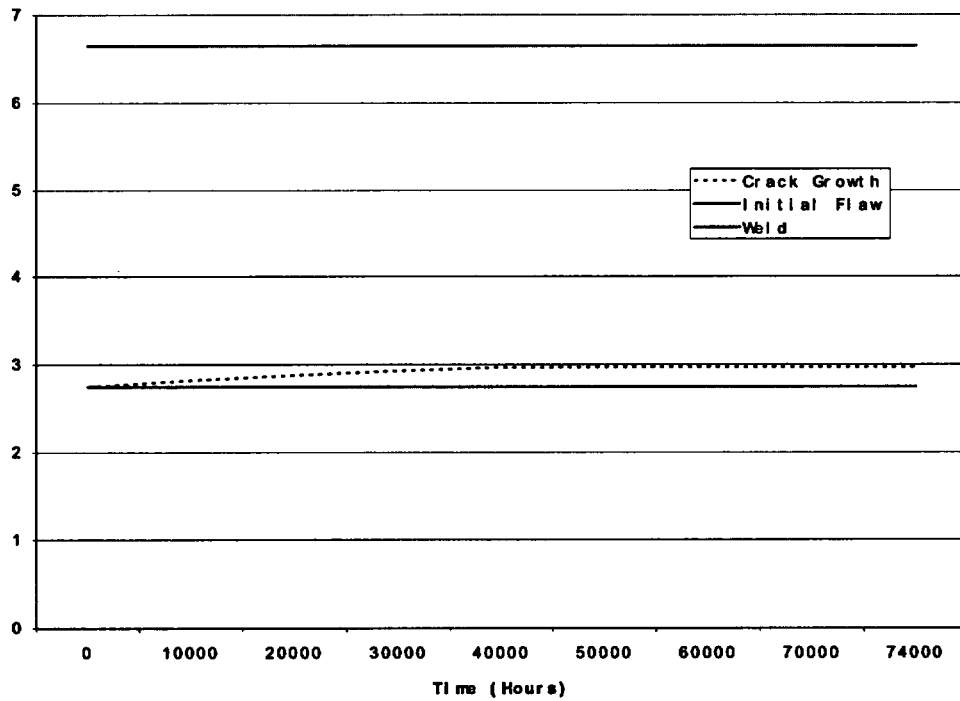


Figure 4-4
Example of Arrested Growth Case (Below Weld Axial Crack)

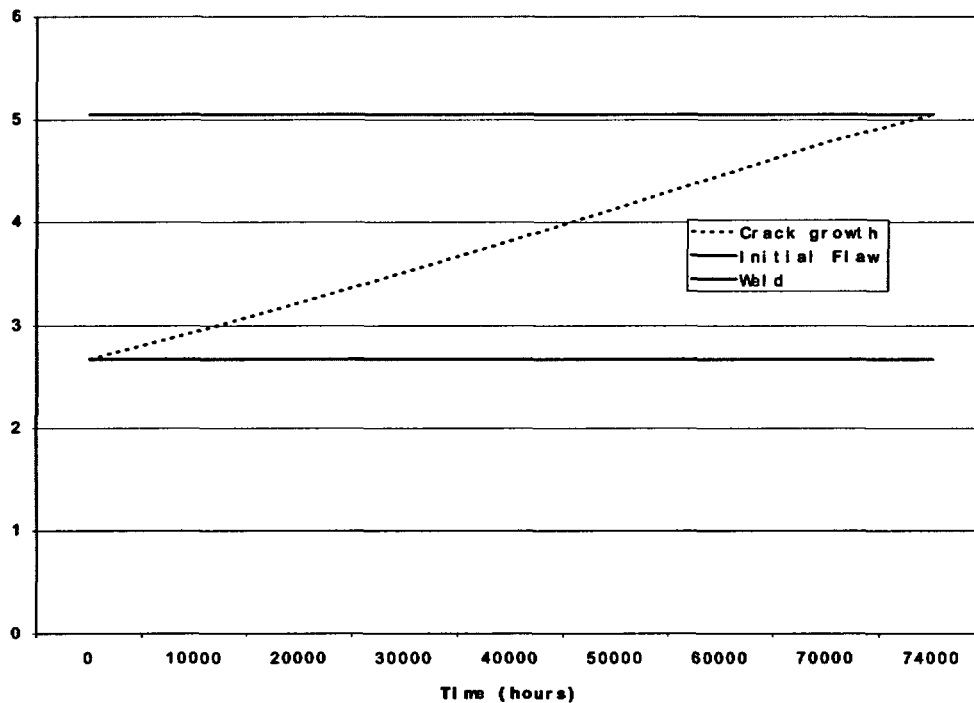


Figure 4-5
Example of Growth Case (Below Weld Axial Crack)

4.2 Growth of Circumferential Cracks Above the Weld

Crack growth correlations for the annulus region above the weld were also developed by the methods of MRP-55 [8] for several assumed head operating temperatures, as summarized in Table 4-2. These crack growth correlations were used with the SI program *pc-CRACK* [7] to perform PWSCC crack growth calculations for initial through-wall circumferential flaws assumed to exist at the top edge of the above-weld inspection zone. As illustrated in Figure 4-2, initial flaw lengths equal to 30° of the nozzle circumference were assumed centered at both the uphill and downhill azimuths.

Previous analyses [9 - 12] developed stress intensity factor results for postulated circumferentially oriented cracks in the critical steepest angle nozzles) of the four characteristic plant types. The results were developed using finite element analysis methods, parametrically varying flaw lengths to determine stress intensity factor versus flaw length. The results are summarized for the four characteristic plant types in Tables 4-4, 4-5, 4-6, and 4-7.

The stress intensity factor results shown in Tables 4-4, 4-5, 4-6, and 4-7 consider an envelope stress distribution of bounding residual and applied stresses above the weld, for the limiting (highest angle) nozzle. The envelope stresses are shown, compared to stresses at the inspection zone boundary for the steepest angle nozzles as well as for smaller angle nozzles in Figure 4-7. It is seen that the envelope stresses assumed clearly bound the applied stresses at the edge of the examination zone.

Table 4-4
**Stress Intensity Factor for Above-Weld Circumferential Flaws for Plant A (B&W Type Plant-
 Envelop Stress Distributions)**

Stress Intensity Factors, K (psi-√in)								
Crack Angle (degrees)	Uphill Side Flaws				Downhill Side Flaws			
	38 DEG.	26 DEG.	18 DEG.	0 DEG.	38 DEG.	26 DEG.	18 DEG.	0 DEG.
30	20141	17334	10711	6780	11227	10142	8985	6780
90	37722	34557	20565	15484	33760	26415	22528	15484
160	51559	47718	32124	26336	68230	53181	42552	26336
180	54337	49976	35163	29383	78168	60404	47890	29383
220	56867	53293	40401	34688	94384	75337	57878	34688
260	59702	56314	44839	38758	115569	90144	65578	38758
300	64773	63152	51868	44166	140472	104128	74058	44166

Table 4-5
**Stress Intensity Factor for Above-Weld Circumferential Flaws for Plant B (W 2-Loop Plant -
 43.5° Nozzle - Envelop Stress Distributions)**

Stress Intensity Factors, K (psi-√in)				
Total Flaw Angle (Degrees)	Maximum		Average	
	Downhill	Uphill	Downhill	Uphill
30	22874	11259	20599	10791
90				
160				
180	85090	30061	79528	26475
220	98756	35937	95130	26392
260	112335	41658	108876	31101
300	126482	52361	113957	40949

Table 4-6
Stress Intensity Factor for Above-Weld Circumferential Flaws for Plant C (W 4-Loop Plant – 48.8° Nozzle - Envelop Stress Distributions)

Stress Intensity Factors, K (psi-√in)				
Total Flaw Angle (Degrees)	Maximum		Average	
	Downhill	Uphill	Downhill	Uphill
30	33672	5436	28790	4942
90	70217	21885	59336	14302
160	95229	23066	84080	21782
180	98532	26524	86557	24115
220	102925	40543	89310	30100
260	109054	52834	92769	38017
300	116987	66244	93453	50009

Table 4-7
Stress Intensity Factor for Above-Weld Circumferential Flaws for Plant D (CE Plant – 49.7° Nozzle - Envelop Stress Distributions)

Stress Intensity Factors, K (psi-√in)				
Total Flaw Angle (Degrees)	Maximum		Average	
	Downhill	Uphill	Downhill	Uphill
30	17939	16439	16514	14873
90	----	----	----	----
160	----	----	----	----
180	70718	84088	62914	73987
220	79030	108473	71523	71713
260	94127	106921	82489	64444
300	124304	104738	98657	62413

The results in the above tables are presented as a function of included flaw angle. These angles correspond to flaw lengths in inches as shown in Table 4-8.

**Table 4-8
Flaw Length Correlations, Degrees and Inches, For Limiting Nozzles**

Crack Length (Degrees)	Crack Length, Inches							
	Plant A 38° Nozzle		Plant B 43.5° Nozzle		Plant C 48.8° Nozzle		Plant D 49.7° Nozzle	
	L	½ L	L	½ L	L	½ L	L	½ L
30	1.062	0.531	1.057	0.528	1.060	0.530	1.077	0.539
90	3.474	1.737	3.368	1.684	3.428	1.714	3.547	1.775
160	6.930	3.465	6.500	3.250	6.731	3.366	7.102	3.551
180	8.108	4.054	7.445	3.722	7.735	3.868	8.192	4.096
220	10.216	5.108	9.321	4.660	9.728	4.864	10.352	5.176
260	12.176	6.088	11.101	5.550	11.603	5.802	12.369	6.185
300	13.900	6.95	12.722	6.361	13.282	6.641	14.142	7.071

In the present analysis, the growth of circumferential through-wall flaws initially assumed to be 30° of circumference to a length of 300° is determined. Analysis details are contained in Reference [13]. 300° corresponds generally to the greatest flaw length that maintains the factors of safety contained in ASME Section XI, IWB-3600. The above-weld flaw growth correlations for 580, 590, 600, 602, and 605°F top head temperatures were used.

Calculations were performed for uphill and downhill-centered flaws, for the limiting (most outboard) nozzles, for the four characteristic plant types.. Results are presented in terms of time required to grow from the assumed initial flaw size (30°) to the allowable size (300°), in Tables 4-9, 4-10, 4-11 and 4-12, in units of both effective full power hours and effective full power years. One EFPY equals 8760 EFPH.

The tabulated stress intensity factor results were input to pc-CRACK [7] in the form of user defined K vs. crack size tables, since the tables are from finite element modeling which gives an inherently more accurate representation of the complex nozzle / vessel head geometry than the crack models in pc-CRACK. The temperature specific PWSCC growth correlations as defined above were used to determine time to allowable for each temperature. A factor of two was applied as shown in Table 4-3, as recommended in MRP-55 [8] to address the more aggressive environment on the CRDM annulus region.

Table 4-11 shows that growth of an initial 30-degree crack in Plant C uphill side of the nozzle is not predicted to grow for any temperature. This is because the applied stress intensity factor at the initial flaw size of 30 degrees (Table 4-6) is predicted to be lower than the threshold value for

growth, $8.19 \text{ ksi}\sqrt{\text{in}}$, as reported in the MRP-55 crack growth formulation [8]. A representative flaw growth plot is presented in Figure 4-6.

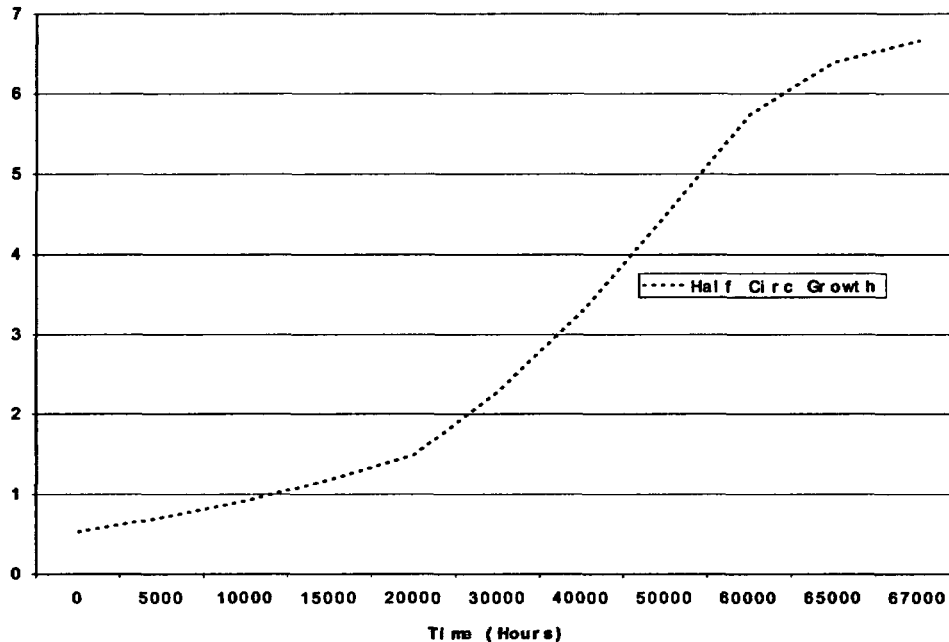


Figure 4-6
Representative Circumferential Crack Growth Case Above Weld

In these analyses, because the assumed flaw is double ended, growth will occur simultaneously from both crack tips. To address this, growth is determined for a half-length flaw (see Table 4-8) to a half-allowable size, using the calculated K vs. a data and the temperature dependent PWSCC crack growth correlations. The resulting initial and final flaw size and growth time is equivalent to a flaw growing at both ends.

Calculations have been performed for various CRDM top head nozzle designs to determine the predicted times for an assumed 30° of circumference flaw to grow to the ASME Section XI allowable flaw size. The calculations were performed for various RPV head operating temperatures ranging from 580°F to 605°F . These calculations predict crack propagation times ranging from 7.65 EFPY for the highest stressed, highest temperature head to as much as 50 EFPY for lower temperature heads. These results are all significantly greater than one refueling cycle, thereby adding further confidence to the inspection zones defined in Section 3.

Table 4-9
Growth Time from 30° to 300° Circumferential Crack
Plant A - 38° Nozzle

TEMPERATURE °F	UPHILL (EFPH)	UPHILL (EFPY)	DOWNHILL (EFPH)	DOWNHILL (EFPY)
580	218000	24.89	205000	23.40
590	168000	19.18	158000	18.04
600	131000	14.95	123000	14.04
602	125000	14.27	117000	13.36
605	116000	13.24	109000	12.44

Table 4-10
Growth Time from 30° to 300° Circumferential Crack
Plant B - 43.5° Nozzle

TEMPERATURE °F	UPHILL (EFPH)	UPHILL (EFPY)	DOWNHILL (EFPH)	DOWNHILL (EFPY)
580	468000	53.4	149000	17.0
590	362000	41.3	115000	13.1
600	281000	32.1	90000	10.3
602	267000	30.5	85000	9.7
605	248000	28.3	79000	9.0

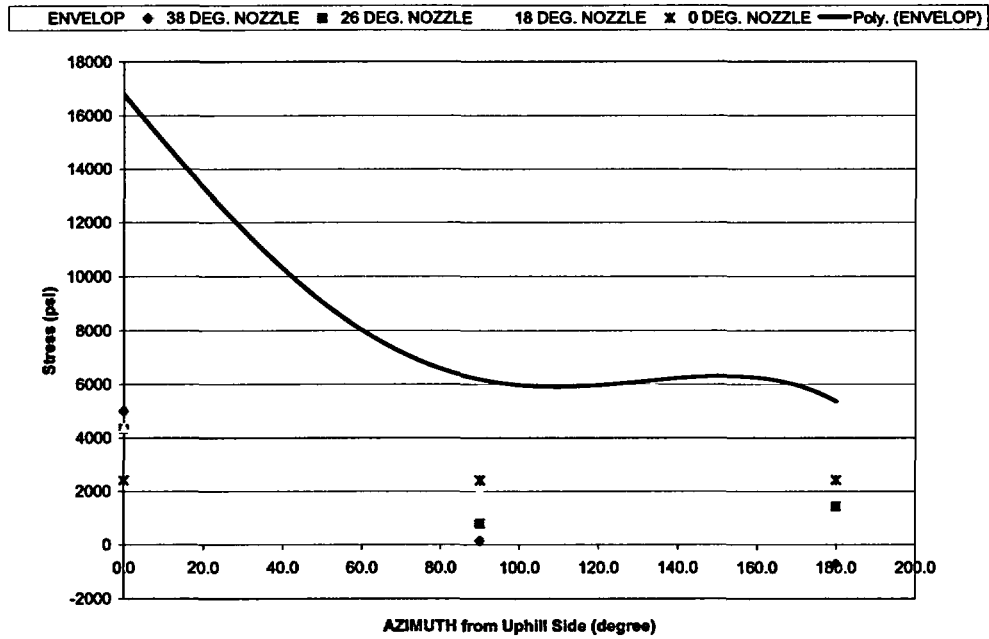
Table 4-11
Growth Time from 30° to 300° Circumferential Crack
Plant C – 48.8° Nozzle

TEMPERATURE °F	UPHILL (EFPH)	UPHILL (EFPY)	DOWNHILL (EFPH)	DOWNHILL (EFPY)
580	no growth	no growth	126000	14.38
590	no growth	no growth	97000	11.07
600	no growth	no growth	76000	8.68
602	no growth	no growth	72000	8.22
605	no growth	no growth	67000	7.65

Table 4-12
Growth Time from 30° to 300° Circumferential Crack
Plant D – 49.7° Nozzle

TEMPERATURE °F	UPHILL (EFPH)	UPHILL (EFPY)	DOWNHILL (EFPH)	DOWNHILL (EFPY)
580	215000	24.54	218000	24.89
590	167000	19.06	169000	19.29
600	130000	14.84	131000	14.95
602	123000	14.04	125000	14.27
605	115000	13.13	116000	13.24

**AVERAGE NORMAL STRESS DISTRIBUTION
38.5 Degree Nozzle, 50 ksi Yield Strength**



**AVERAGED NORMAL STRESS DISTRIBUTION
43.5 Degree Nozzle, 58 ksi Yield Strength**

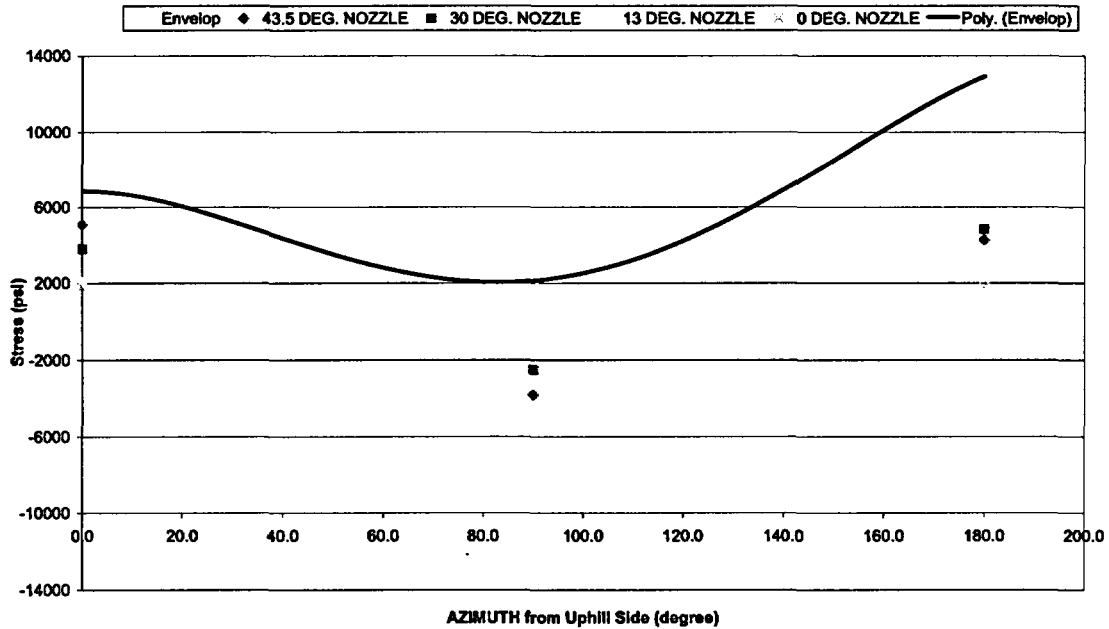


**Figure 4-7
Envelope Stresses Compared to Stresses at Edge of Inspection Zone**

5

COMPARISON TO PAST INSPECTION RESULTS

Finally, a review of past top head inspection results for U.S. PWRs was performed to determine if flaws were found in prior inspections that were completely outside of the new inspection zone definition, and would thus be missed if the revised inspection zones were implemented. Figure 5-1 presents a plot of the past inspection data for the CRDMs for several plants in the U.S.

It should be noted that weld height is not represented in the vertical axis; all distances on the vertical axis represent distances above the top and below the bottom of the weld. Therefore, flaws that begin (or end) anywhere within the weld are shown as beginning (or ending) at the zero-inch line. Similarly, flaws that are completely contained within the weld are shown as a point on the zero inch line.

The Figure 5-1 plot shows that of the 237 data points studied, 3 flaws (shown in green squares) begin at a distance greater than 0.75 inch above the weld and proceed away from the weld. Similarly, 22 flaws (shown in red circles) begin at a distance greater than 0.75 inch below the weld and proceed away from the weld. A portion of each of the remaining 212 flaws is within the 0.75-inch distance above or below the weld. To determine if the 25 flaws would be encompassed in the area between horizontal scans at 0.75 inch above the top of the weld on the uphill side and 0.75 inch below the bottom of the weld on the downhill side (horizontal scan region), azimuthal locations of these 25 flaws were examined further. It was found that a portion of all 25 flaws are within the recommended inspection zone.

Therefore, in the prior inspections dataset examined, all flaws were found to be within the new inspection zone definition, and would thus be detected if the revised inspection zones were implemented. This dataset represents a significant cross section of the CRDM/CEDM inspection findings in U.S. PWRs.

Figure 5.1 Flaw Area Outside of Weld

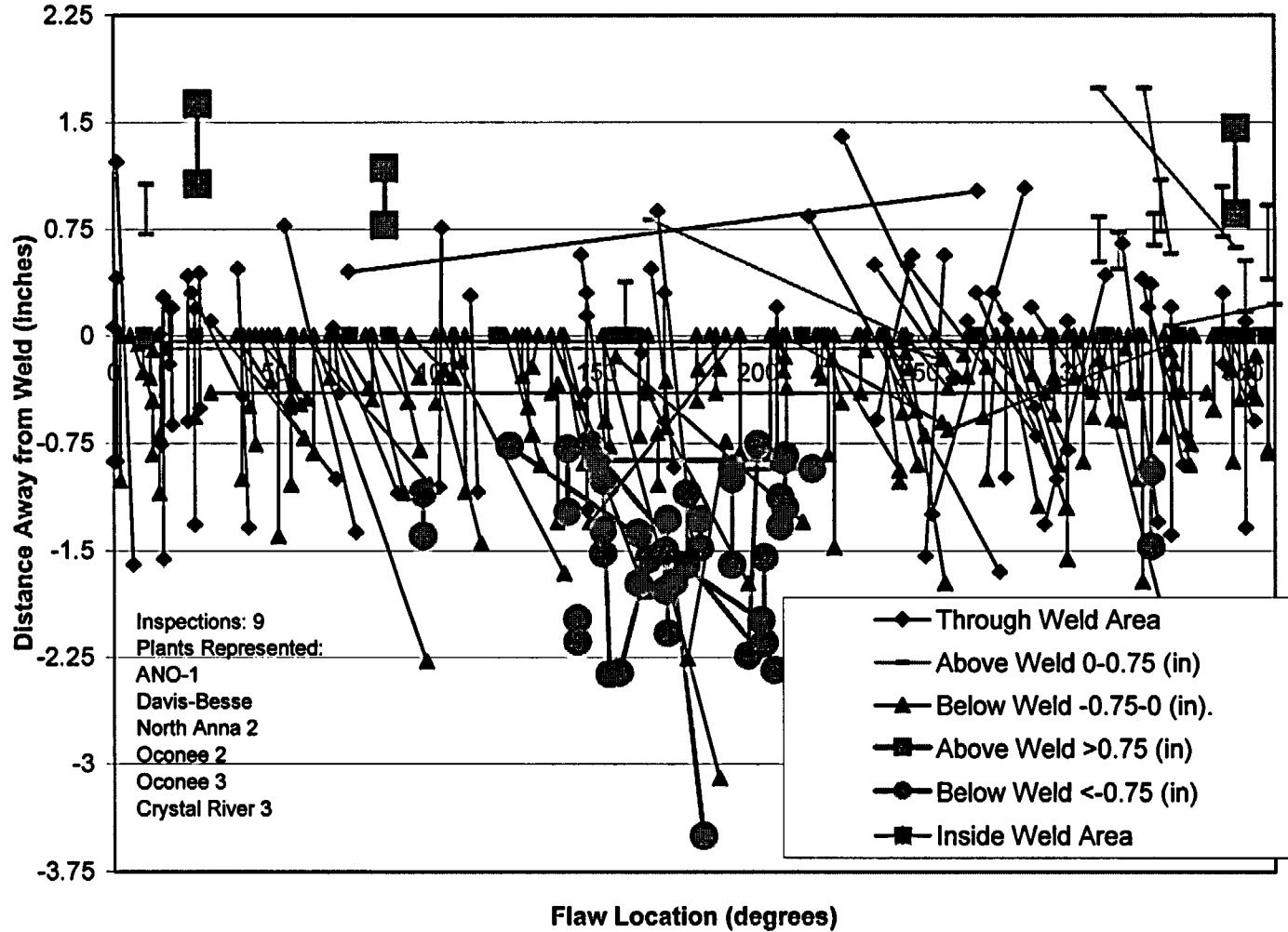


Figure 5-1
Flaw Area Outside of Weld

6

CONCLUSIONS

This report contains a generic technical evaluation to determine a practical examination zone for PWR top head inspections which will provide an acceptable level of quality and safety. It addresses extent of examination both above the top and below the bottom of the J-groove weld. The evaluation considers stresses in a group of characteristic plants that reasonably bound the fleet of U.S. PWRs from the standpoint of the important factors that contribute to nozzle residual and operating stresses. Plots of stress versus distance above and below the J-groove weld are developed for several nozzles in these plants. Inspection zones are then defined, beyond which the stresses decay significantly, to levels at which primary water stress corrosion cracking (PWSCC) is considered highly unlikely. Then, assuming (non-mechanistically) that cracks form in the uninspected regions up to and impinging upon the proposed inspection zones, fracture mechanics calculations are performed to demonstrate that such cracks would not propagate to an unacceptable size for several operating cycles in plants of various RPV head designs and operating temperatures. Finally, NDE data are reviewed and presented to demonstrate the effectiveness of the proposed examination zone with respect to prior inspection results for U.S. PWR top head nozzles.

The results of this evaluation support an inspection zone, illustrated schematically in Figure 3-1 of this report, in which the short sides (a_{up} and b_{dn} in Fig. 3-1) are equal to 0.75 in. The long sides of the inspection zone (a_{dn} and b_{up} in Fig. 3-1) are dependent on nozzle angle, but in all cases are bounded by horizontal scans encompassing the 0.75 in. short side dimensions. The report establishes a reasonable target stress value (20 ksi), below which PWSCC is extremely remote, and demonstrates that in all but a few isolated cases, the inspection zone, as defined above, envelopes locations with stresses above this stress level. In no case does the examination zone exclude locations with stresses higher than 70% of the material yield strength. The report also includes PWSCC growth calculations of postulated large flaws that could be overlooked due to unexamined regions, to demonstrate that such flaws, either above or below the weld, would not grow to unacceptable sizes in several operating cycles. Finally, review of prior plant inspection data from a large cross-section of U.S. PWRs revealed that, of 237 flaw indications reported in these inspections all flaws would have been detected had the inspections been limited to just the proposed examination zones.

7

REFERENCES

- 1.0 K. M. Boursier et al (EDF), "Effect of Strain Rate on SCC in High Temperature Primary Water, Comparison between Alloys 690 and 600, ANS 11th Environmental Degradation Meeting, August, 2003/
- 2.0 P. Scott, "Prediction of Alloy 600 Component Failures in RWP System," Research Topical Symposia Part 1 – Life Prediction of Structures Subject to Environmental Degradation, NACE, Houston (1997)
- 3.0 Dominion Engineering, Inc. Calculation No. C-4142-00-2, Rev. 0, "Plant A CRDM Stress Analysis," 8/29/01, (Proprietary)
- 4.0 Dominion Engineering, Inc. Calculation No. C-7612-00-1, Rev. 0, "Plant B CRDM Stress Analysis," October 31, 2001, (Proprietary)
- 5.0 Dominion Engineering, Inc. Calculation No. R-7613-00-1, Rev. 0, "Plant C Fall 2002 CRDM Repair Analysis", January 2003, (Proprietary)
- 6.0 Dominion Engineering, Inc. Calculation No. C-7736-00-8, Rev. 0, "Plant D CEDM and ICI Stress Analysis – Alternate Element Mesh", 03/08/02, (Proprietary)
- 7.0 Structural Integrity Associates, pc-CRACK for Windows, version 3.1-98348
- 8.0 Materials Reliability Program (MRP), "Crack Growth Rates for Evaluating Primary Water Stress Corrosion Cracking (PWSCC) of Thick-Wall Alloy 600 Material", MRP-55, Revision 1, November 2002. EPRI Proprietary
- 9.0 Structural Integrity Associates, Inc. Calculation No. W-EPRI-182-303, "Deterministic Fracture Mechanics Evaluation of Top Head CRDM Nozzle with Through-Wall Flaw – B&W Type Plant A," 3/26/03 (Contains Vendor Proprietary Information)
- 10.0 Structural Integrity Associates, Inc. Calculation No. W-EPRI-182-309 "Deterministic Fracture Mechanics Evaluation of Westinghouse 2-Loop Top Head CRDM Nozzle with Through-Wall Flaw, Plant B," 7/22/03 (Contains Vendor Proprietary Information)
- 11.0 Structural Integrity Associates, Inc. Calculation No. W-EPRI-182-304, "Deterministic Fracture Mechanics Evaluation of Top Head CRDM Nozzle with Through-Wall Flaw - Westinghouse Type Plant C, 5/09/03, (Contains Vendor Proprietary Information)

References

- 12.0 Structural Integrity Associates Calculation EPRI-182Q-305, "Deterministic Fracture Mechanics Evaluation of Top Head CRDM Nozzle with Through-Wall Flaw - CE Type Plant D", June 2003, (Contains Vendor Proprietary Information)
- 13.0 Structural Integrity Associates Calculation EPRI-182Q-307, "Deterministic Fracture Mechanics Crack Growth Calculations – Circ Flaws Above Weld", 9/05/03
- 14.0 Structural Integrity Associates Calculation EPRI-182Q-310, "Deterministic Fracture Mechanics Crack Growth Calculations – Axial Flaws Below Weld", 9/05/03

A

APPENDIX A

**Content Deleted – MRP/EPRI
Proprietary Material**

**Figure A-1
Plant A (B&W) 38° Nozzle downhill Hoop Stress**

**Content Deleted – MRP/EPRI
Proprietary Material**

Figure A-2
Plant A (B&W) 38° Nozzle downhill Axial Stress

**Content Deleted – MRP/EPRI
Proprietary Material**

Figure A-3
Plant A (B&W) 38° Nozzle sidehill Hoop Stress

**Content Deleted – MRP/EPRI
Proprietary Material**

Figure A-4
Plant A (B&W) 38° Nozzle sidehill Axial Stress

**Content Deleted – MRP/EPRI
Proprietary Material**

Figure A-5
Plant A (B&W) 38° Nozzle uphill Hoop Stress

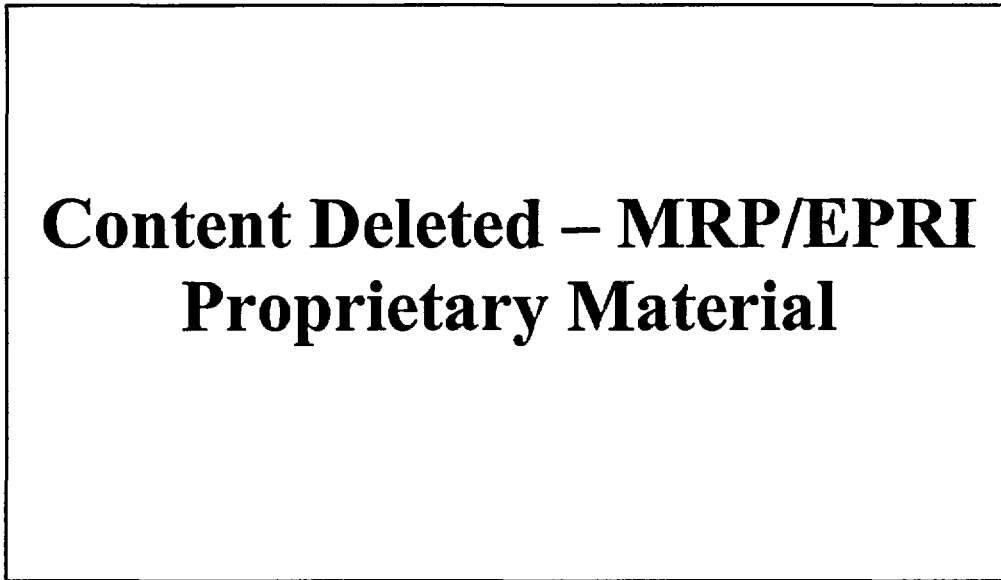


**Figure A-6
Plant A (B&W) 38° Nozzle uphill Axial Stress**

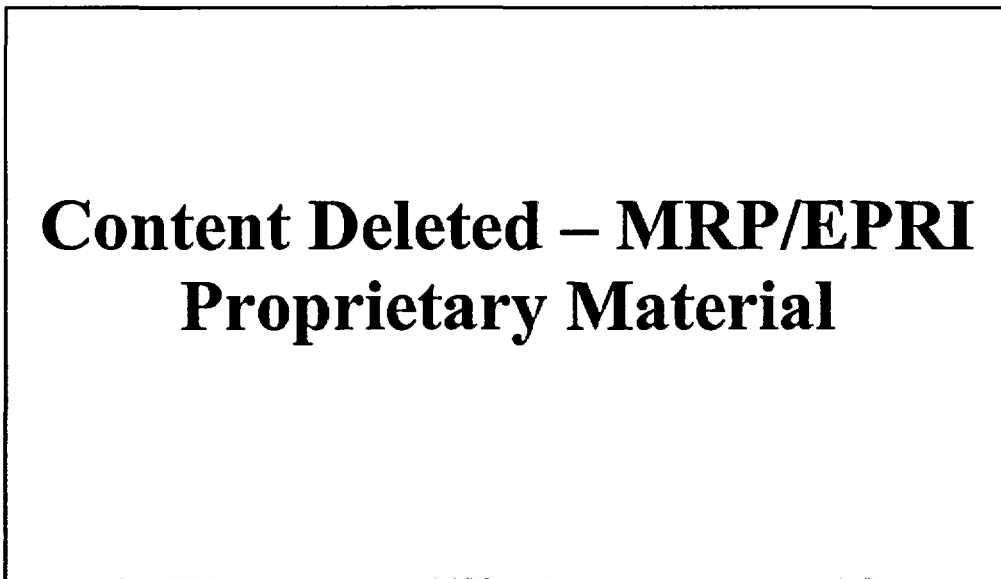


**Figure A-7
Plant A (B&W) 26° Nozzle downhill Hoop Stress**

**Content Deleted – MRP/EPRI
Proprietary Material**

**Figure A-8
Plant A (B&W) 26° Nozzle downhill Axial Stress**

**Content Deleted – MRP/EPRI
Proprietary Material**

**Figure A-9
Plant A (B&W) 26° Nozzle sidehill Hoop Stress**

**Content Deleted – MRP/EPRI
Proprietary Material**

Figure A-10
Plant A (B&W) 26° Nozzle sidehill Axial Stress

**Content Deleted – MRP/EPRI
Proprietary Material**

Figure A-11
Plant A (B&W) 26° Nozzle uphill Hoop Stress

**Content Deleted – MRP/EPRI
Proprietary Material**

**Figure A-12
Plant A (B&W) 26° Nozzle uphill Axial Stress**

**Content Deleted – MRP/EPRI
Proprietary Material**

**Figure A-13
Plant A (B&W) 18° Nozzle downhill Hoop Stress**

**Content Deleted – MRP/EPRI
Proprietary Material**

Figure A-14
Plant A (B&W) 18° Nozzle downhill Axial Stress

**Content Deleted – MRP/EPRI
Proprietary Material**

Figure A-15
Plant A (B&W) 18° Nozzle sidehill Hoop Stress

**Content Deleted – MRP/EPRI
Proprietary Material**

Figure A-16
Plant A (B&W) 18° Nozzle sidehill Axial Stress

**Content Deleted – MRP/EPRI
Proprietary Material**

Figure A-17
Plant A (B&W) 18° Nozzle uphill Hoop Stress

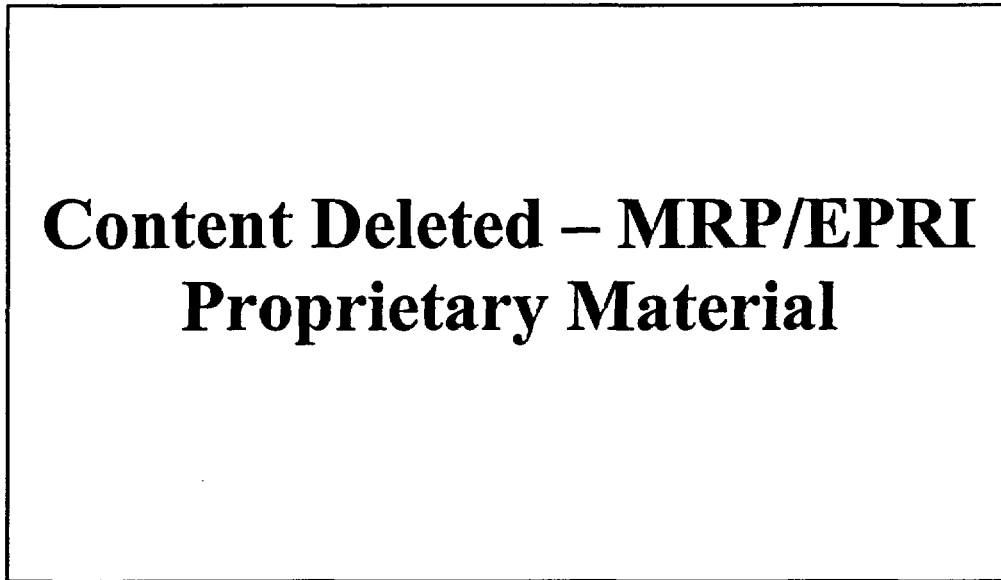


**Figure A-18
Plant A (B&W) 18° Nozzle uphill Axial Stress**

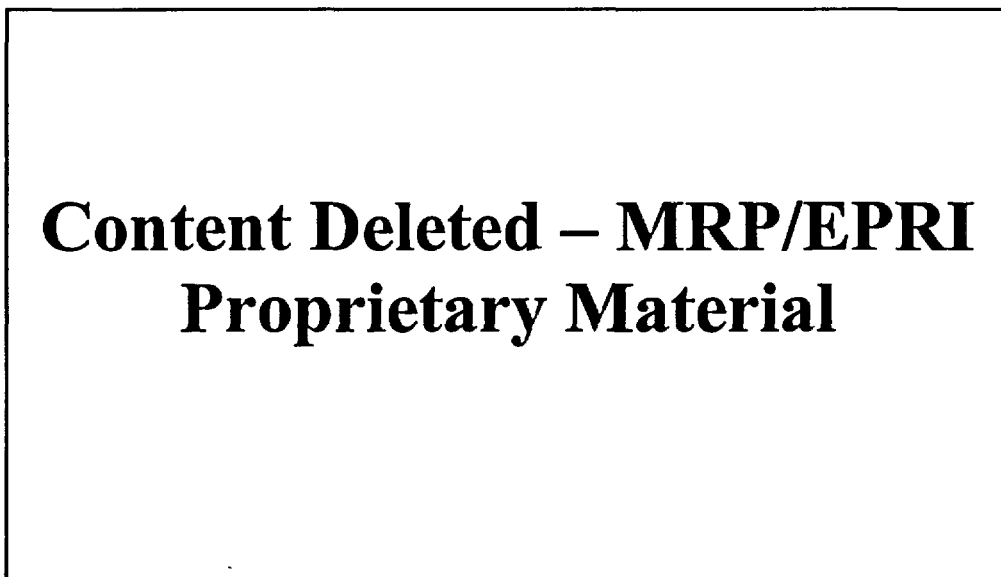


**Figure A-19
Plant A (B&W) 0° Nozzle downhill Hoop Stress**

**Content Deleted – MRP/EPRI
Proprietary Material**

**Figure A-20
Plant A (B&W) 0° Nozzle downhill Axial Stress**

**Content Deleted – MRP/EPRI
Proprietary Material**

**Figure A-21
Plant A (B&W) 0° Nozzle sidehill Hoop Stress**

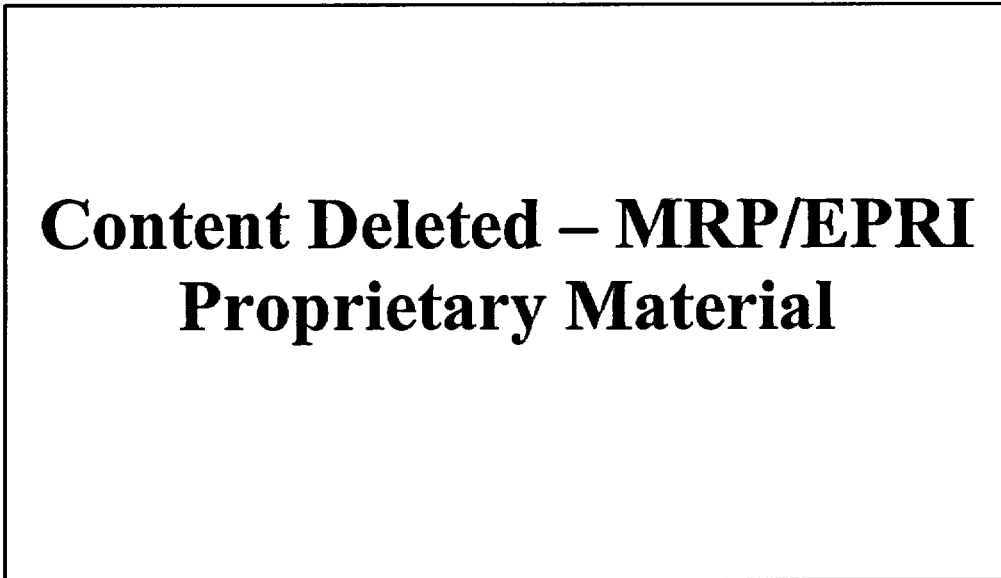


**Figure A-22
Plant A (B&W) 0° Nozzle sidehill Axial Stress**

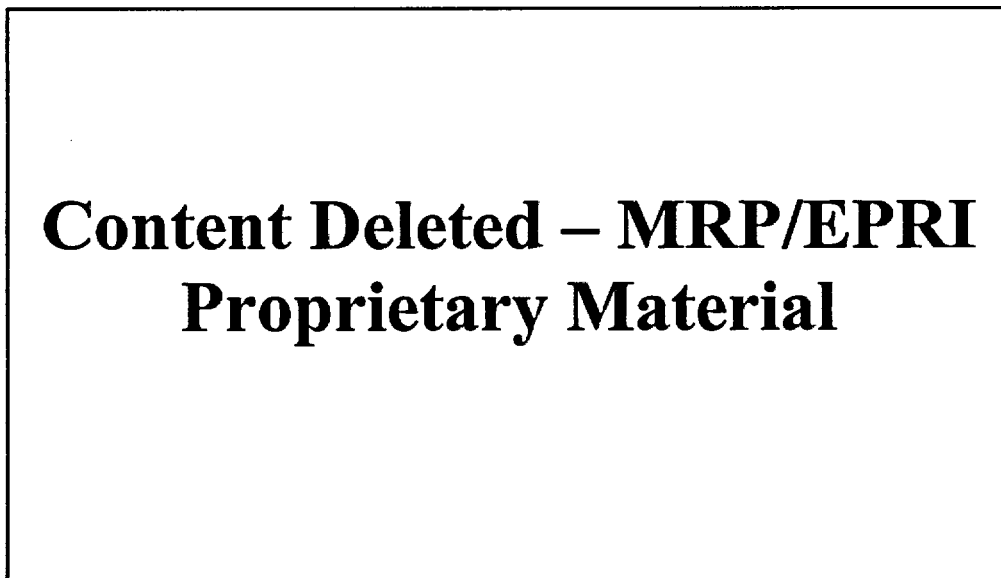


**Figure A-23
Plant A (B&W) 0° Nozzle uphill Hoop Stress**

**Content Deleted – MRP/EPRI
Proprietary Material**

**Figure A-24
Plant A (B&W) 0° Nozzle uphill Axial Stress**

**Content Deleted – MRP/EPRI
Proprietary Material**

**Figure A-25
Plant B (Westinghouse 2-loop) 43° Nozzle downhill Hoop Stress**

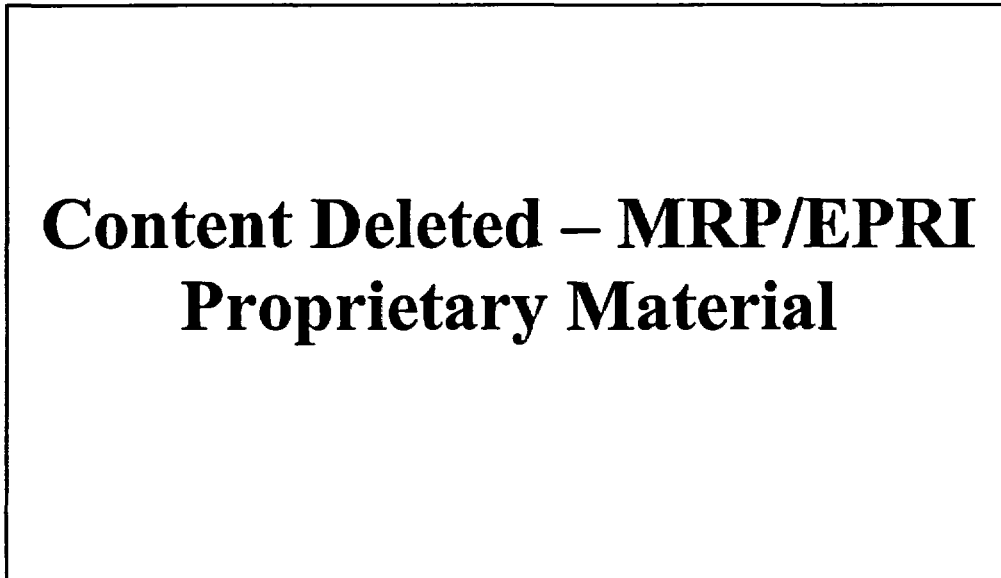


Figure A-26
Plant B (Westinghouse 2-loop) 43° Nozzle downhill Axial Stress

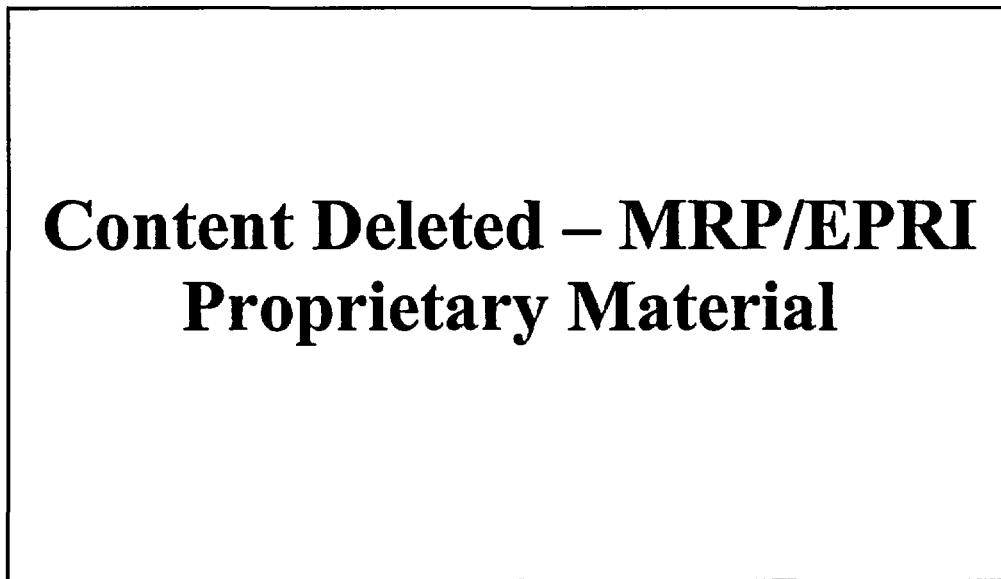


Figure A-27
Plant B (Westinghouse 2-loop) 43° Nozzle sidehill Hoop Stress

**Content Deleted – MRP/EPRI
Proprietary Material**

**Figure A-28
Plant B (Westinghouse 2-loop) 43° Nozzle sidehill Axial Stress**

**Content Deleted – MRP/EPRI
Proprietary Material**

**Figure A-29
Plant B (Westinghouse 2-loop) 43° Nozzle uphill Hoop Stress**

**Content Deleted – MRP/EPRI
Proprietary Material**

**Figure A-30
Plant B (Westinghouse 2-loop) 43° Nozzle uphill Axial Stress**

**Content Deleted – MRP/EPRI
Proprietary Material**

**Figure A-31
Plant B (Westinghouse 2-loop) 30° Nozzle downhill Hoop Stress**

**Content Deleted – MRP/EPRI
Proprietary Material**

**Figure A-32
Plant B (Westinghouse 2-loop) 30° Nozzle downhill Axial Stress**

**Content Deleted – MRP/EPRI
Proprietary Material**

**Figure A-33
Plant B (Westinghouse 2-loop) 30° Nozzle sidehill Hoop Stress**

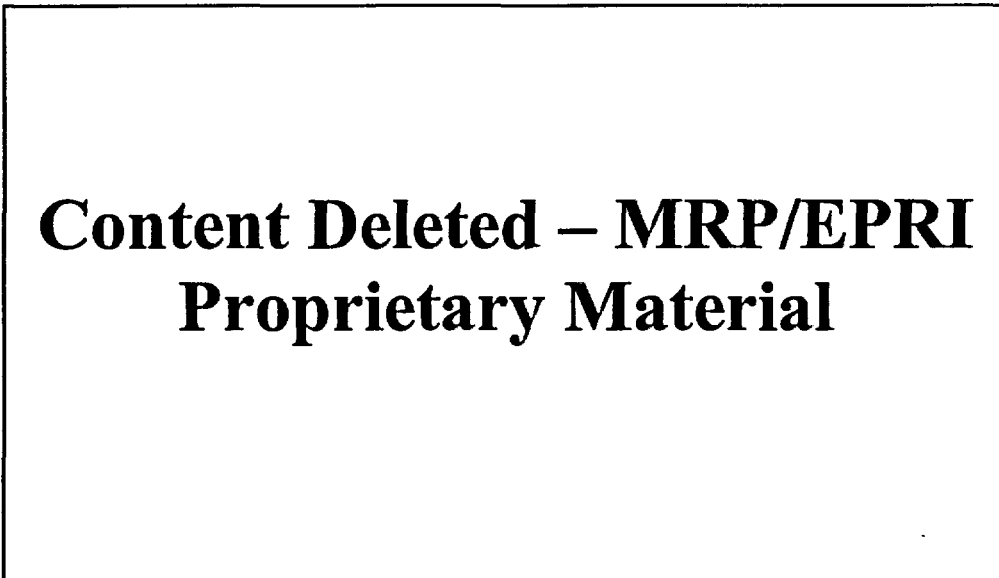


**Figure A-34
Plant B (Westinghouse 2-loop) 30° Nozzle sidehill Axial Stress**

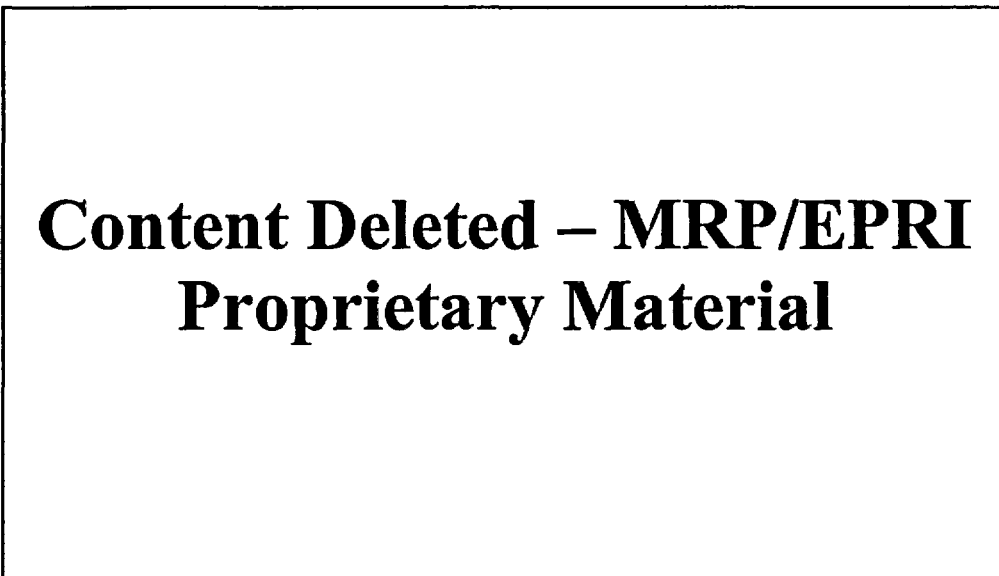


**Figure A-35
Plant B (Westinghouse 2-loop) 30° Nozzle uphill Hoop Stress**

**Content Deleted – MRP/EPRI
Proprietary Material**

Figure A-36
Plant B (Westinghouse 2-loop) 30° Nozzle uphill Axial Stress

**Content Deleted – MRP/EPRI
Proprietary Material**

Figure A-37
Plant B (Westinghouse 2-loop) 13° Nozzle downhill Hoop Stress

**Content Deleted – MRP/EPRI
Proprietary Material**

**Figure A-38
Plant B (Westinghouse 2-loop) 13° Nozzle downhill Axial Stress**

**Content Deleted – MRP/EPRI
Proprietary Material**

**Figure A-39
Plant B (Westinghouse 2-loop) 13° Nozzle sidehill Hoop Stress**

**Content Deleted – MRP/EPRI
Proprietary Material**

**Figure A-40
Plant B (Westinghouse 2-loop) 13° Nozzle sidehill Axial Stress**

**Content Deleted – MRP/EPRI
Proprietary Material**

**Figure A-41
Plant B (Westinghouse 2-loop) 13° Nozzle uphill Hoop Stress**

**Content Deleted – MRP/EPRI
Proprietary Material**

Figure A-42
Plant B (Westinghouse 2-loop) 13° Nozzle uphill Axial Stress

**Content Deleted – MRP/EPRI
Proprietary Material**

Figure A-43
Plant B (Westinghouse 2-loop) 0° Nozzle downhill Hoop Stress

**Content Deleted – MRP/EPRI
Proprietary Material**

**Figure A-44
Plant B (Westinghouse 2-loop) 0° Nozzle downhill Axial Stress**

**Content Deleted – MRP/EPRI
Proprietary Material**

**Figure A-45
Plant B (Westinghouse 2-loop) 0° Nozzle sidehill Hoop Stress**

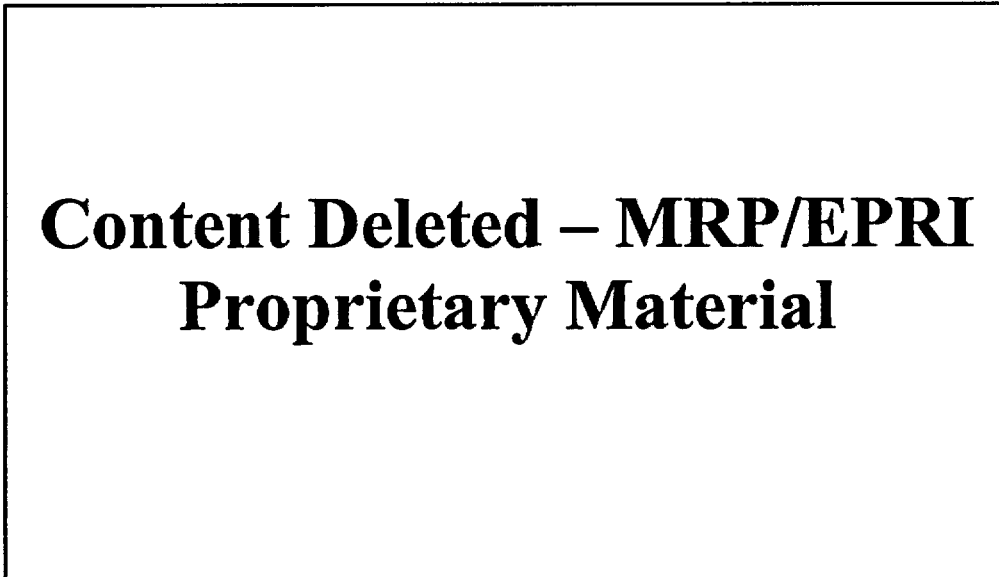


**Figure A-46
Plant B (Westinghouse 2-loop) 0° Nozzle sidehill Axial Stress**

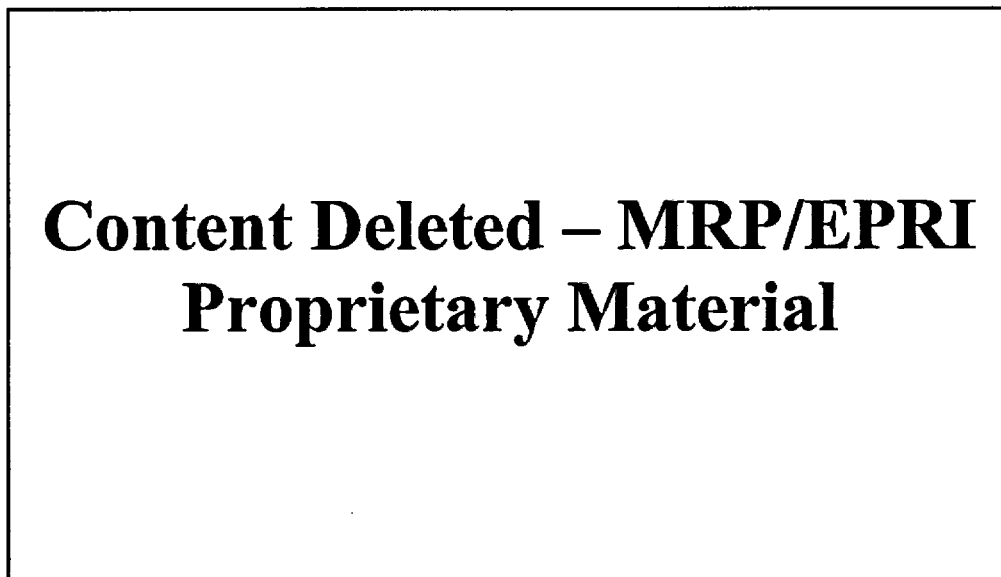


**Figure A-47
Plant B (Westinghouse 2-loop) 0° Nozzle uphill Hoop Stress**

**Content Deleted – MRP/EPRI
Proprietary Material**

**Figure A-48
Plant B (Westinghouse 2-loop) 0° Nozzle uphill Axial Stress**

**Content Deleted – MRP/EPRI
Proprietary Material**

**Figure A-49
Plant C (Westinghouse 4-loop) 48° Nozzle downhill Hoop Stress**

**Content Deleted – MRP/EPRI
Proprietary Material**

Figure A-50
Plant C (Westinghouse 4-loop) 48° Nozzle downhill Axial Stress

**Content Deleted – MRP/EPRI
Proprietary Material**

Figure A-51
Plant C (Westinghouse 4-loop) 48° Nozzle sidehill Hoop Stress

**Content Deleted – MRP/EPRI
Proprietary Material**

**Figure A-52
Plant C (Westinghouse 4-loop) 48° Nozzle sidehill Axial Stress**

**Content Deleted – MRP/EPRI
Proprietary Material**

**Figure A-53
Plant C (Westinghouse 4-loop) 48° Nozzle uphill Hoop Stress**

**Content Deleted – MRP/EPRI
Proprietary Material**

**Figure A-54
Plant C (Westinghouse 4-loop) 48° Nozzle uphill Axial Stress**

**Content Deleted – MRP/EPRI
Proprietary Material**

**Figure A-55
Plant D (CE) 49° Nozzle downhill Hoop Stress**

**Content Deleted – MRP/EPRI
Proprietary Material**

Figure A-56
Plant D (CE) 49° Nozzle downhill Axial Stress

**Content Deleted – MRP/EPRI
Proprietary Material**

Figure A-57
Plant D (CE) 49° Nozzle sidehill Hoop Stress

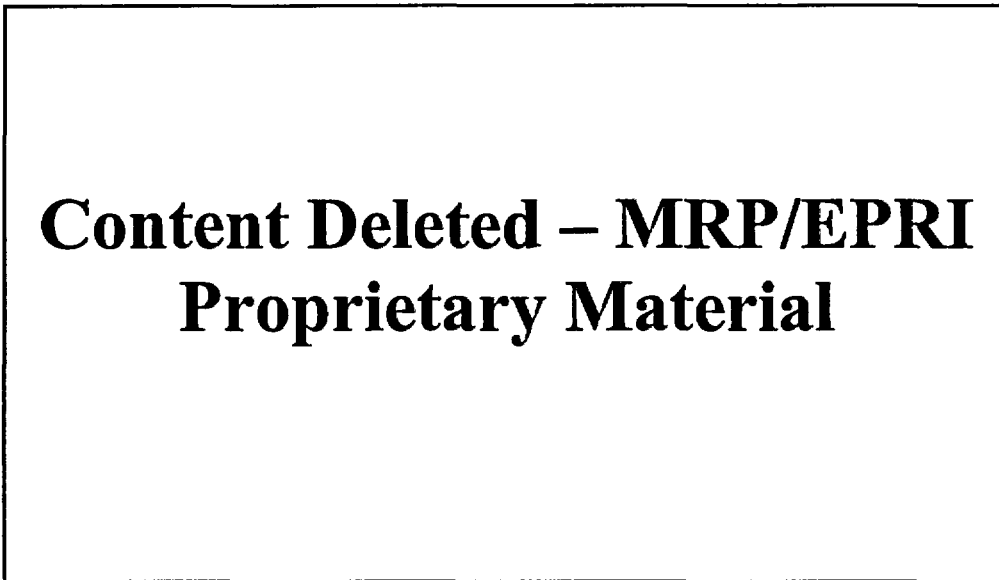


Figure A-58
Plant D (CE) 49° Nozzle sidehill Axial Stress

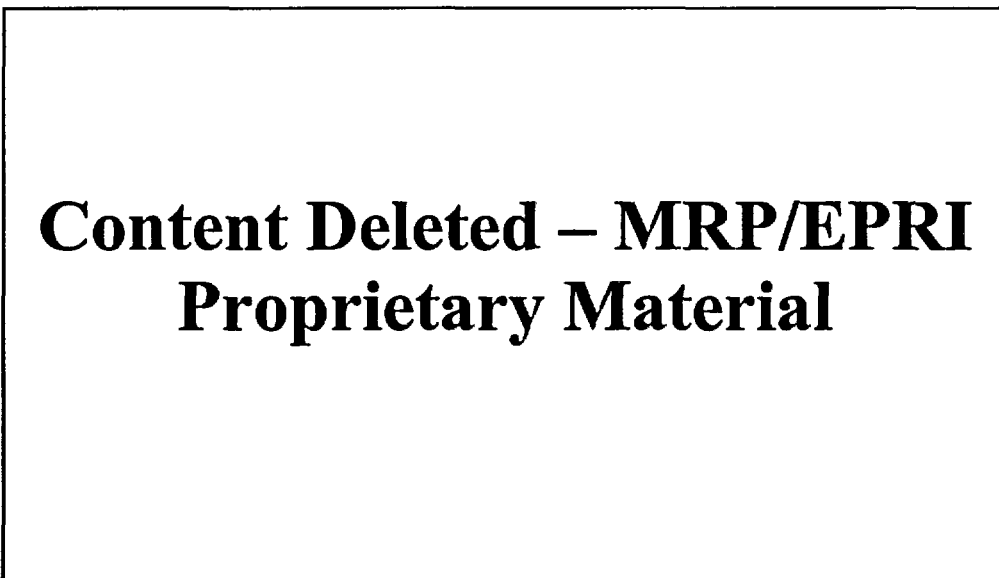


Figure A-59
Plant D (CE) 49° Nozzle uphill Hoop Stress

**Content Deleted – MRP/EPRI
Proprietary Material**

Figure A-60
Plant D (CE) 49° Nozzle uphill Axial Stress

**Content Deleted – MRP/EPRI
Proprietary Material**

Figure A-61
Plant D (CE) 8° Nozzle downhill Hoop Stress

**Content Deleted – MRP/EPRI
Proprietary Material**

Figure A-62
Plant D (CE) 8° Nozzle downhill Axial Stress

**Content Deleted – MRP/EPRI
Proprietary Material**

Figure A-63
Plant D (CE) 8° Nozzle sidehill Hoop Stress

**Content Deleted – MRP/EPRI
Proprietary Material**

**Figure A-64
Plant D (CE) 8° Nozzle sidehill Axial Stress**

**Content Deleted – MRP/EPRI
Proprietary Material**

**Figure A-65
Plant D (CE) 8° Nozzle uphill Hoop Stress**

**Content Deleted – MRP/EPRI
Proprietary Material**

Figure A-66
Plant D (CE) 8° Nozzle uphill Axial Stress

**Content Deleted – MRP/EPRI
Proprietary Material**

Figure A-67
Plant D (CE) ICI Nozzle downhill Hoop Stress

**Content Deleted – MRP/EPRI
Proprietary Material**

**Figure A-68
Plant D (CE) ICI Nozzle downhill Axial Stress**

**Content Deleted – MRP/EPRI
Proprietary Material**

**Figure A-69
Plant D (CE) ICI Nozzle sidehill Hoop Stress**

**Content Deleted – MRP/EPRI
Proprietary Material**

Figure A-70
Plant D (CE) ICI Nozzle sidehill Axial Stress

**Content Deleted – MRP/EPRI
Proprietary Material**

Figure A-71
Plant D (CE) ICI Nozzle uphill Hoop Stress

**Content Deleted – MRP/EPRI
Proprietary Material**

**Figure A-72
Plant D (CE) ICI Nozzle uphill Axial Stress**

B

APPENDIX B

**Content Deleted – MRP/EPRI
Proprietary Material**

**Figure B-1
Inspection Zone Distances that Envelopes > 20 ksi Stress Regions
Plant A (B&W) 38° Nozzle**

**Content Deleted – MRP/EPRI
Proprietary Material**

**Figure B-2
Inspection Zone Distances that Envelopes > 20 ksi Stress Regions
Plant A (B&W) 26° Nozzle**

**Content Deleted – MRP/EPRI
Proprietary Material**

**Figure B-3
Inspection Zone Distances that Envelopes > 20 ksi Stress Regions
Plant A (B&W) 18° Nozzle**

**Content Deleted – MRP/EPRI
Proprietary Material**

**Figure B-4
Inspection Zone Distances that Envelopes > 20 ksi Stress Regions
Plant A (B&W) 0° Nozzle**

**Content Deleted – MRP/EPRI
Proprietary Material**

**Figure B-5
Inspection Zone Distances that Envelopes > 20 ksi Stress Regions
Plant B (Westinghouse 2-loop) 43° Nozzle**

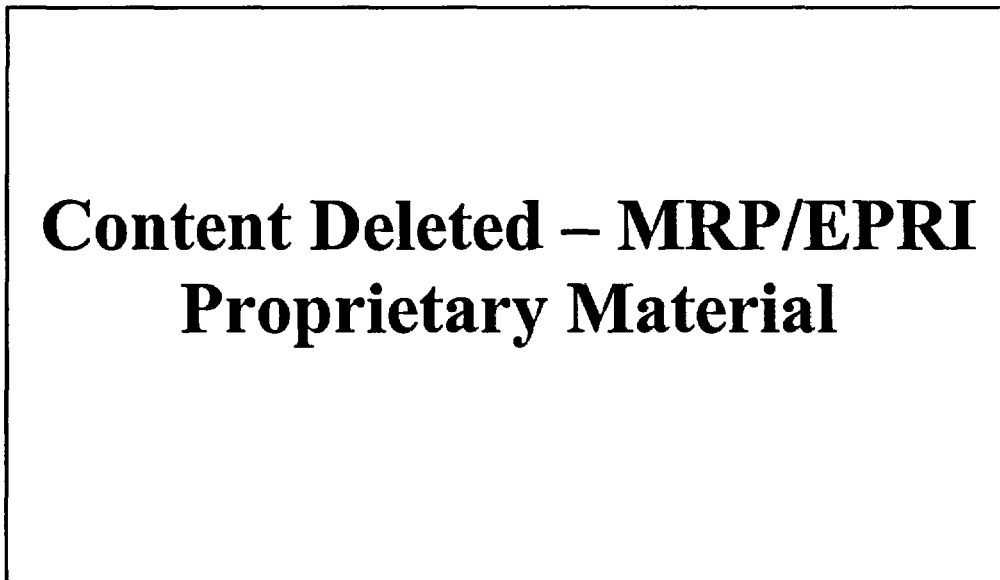


**Figure B-6
Inspection Zone Distances that Envelopes > 20 ksi Stress Regions
Plant B (Westinghouse 2-loop) 30° Nozzle**

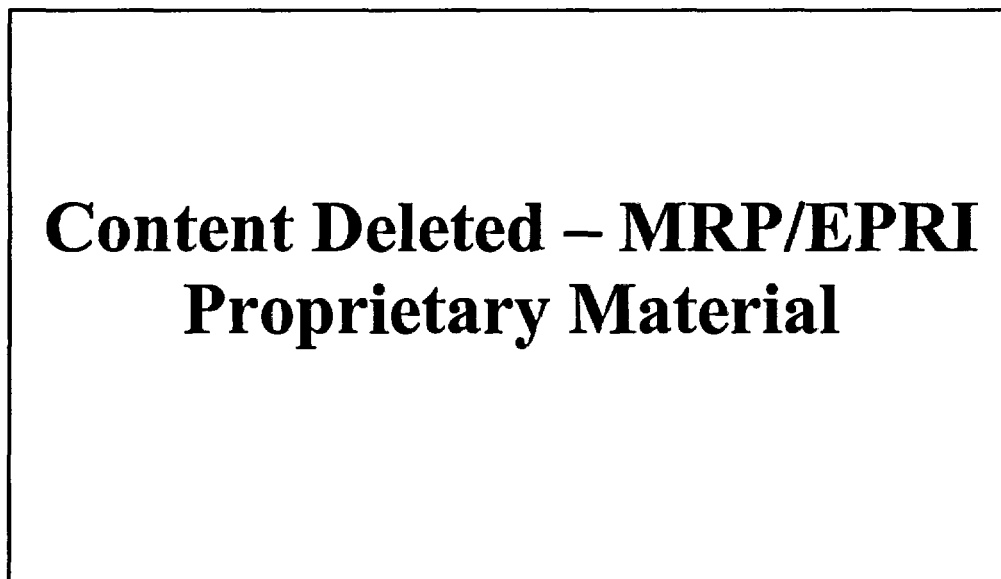


**Figure B-7
Inspection Zone Distances that Envelopes > 20 ksi Stress Regions
Plant B (Westinghouse 2-loop) 13° Nozzle**

**Content Deleted – MRP/EPRI
Proprietary Material**

**Figure B-8
Inspection Zone Distances that Envelopes > 20 ksi Stress Regions
Plant B (Westinghouse 2-loop) 0° Nozzle**

**Content Deleted – MRP/EPRI
Proprietary Material**

**Figure B-9
Inspection Zone Distances that Envelopes > 20 ksi Stress Regions
Plant C (Westinghouse 4-loop) 48° Nozzle**

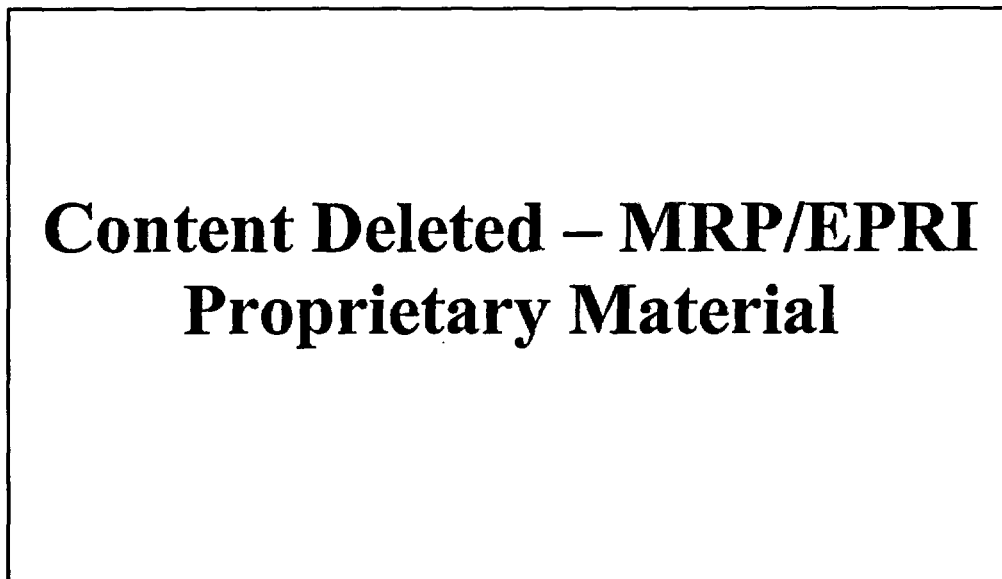


**Figure B-10
Inspection Zone Distances that Envelopes > 20 ksi Stress Regions
Plant D (CE) 49° Nozzle**

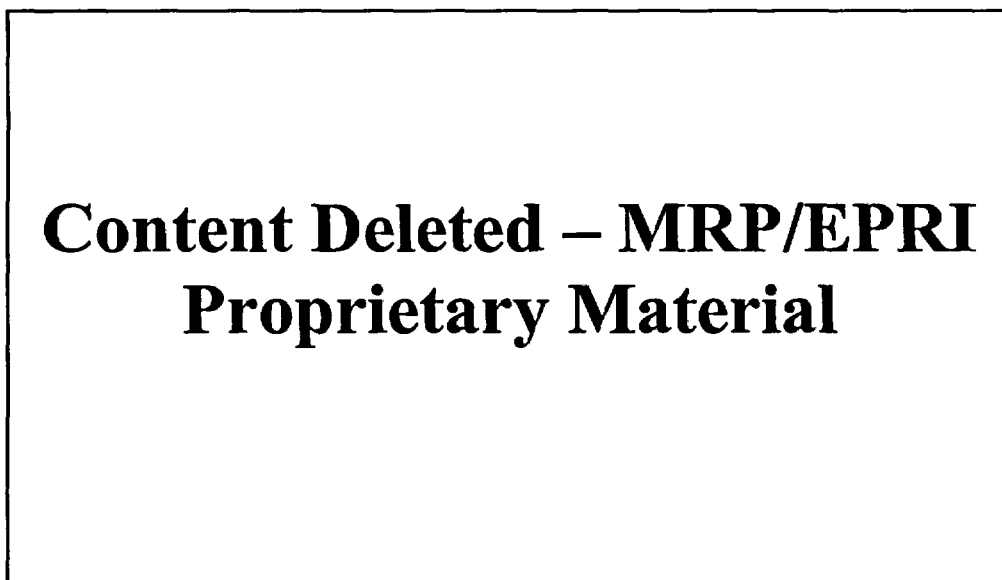


**Figure B-11
Inspection Zone Distances that Envelopes > 20 ksi Stress Regions
Plant D (CE) 8° Nozzle**